Journal of Statistical Physics, Vol. 21, No. 4, 1979

Theory of Irreversible Processes in Nonequilibrium Quantum Systems. I. General Formalism

Nobuhiko Mishima,[1] Tomio Yamakoshi Petrosky,[2] and Ryoji Suzuki[2]

Received January 11, 1979

The theory of Van Hove for nonequilibrium quantum statistical mechanics is extensively reformulated in terms of a superspace (a kind of operator space). This reformulation enables us to introduce a diagrammatic method which makes it convenient to deal with practical problems in physical systems. In our formalism, quantum statistical effects are considered on the basis of a systematic rule for the contraction technique. A complicated statistical effect in boson or fermion systems can be treated by starting with a simple unsymmetrized formalism in the Boltzmann statistics.

KEY WORDS: Two-resolvent method; compensative relation; product and ordered product representations; moving contraction; internal and external contractions.

1. INTRODUCTION

Since the generalized master equation was first derived by Van Hove,[1] remarkable progress has been made in the study of irreversible processes in nonequilibrium statistical mechanics. Much of this progress has been achieved by the Brussels school led by Prigogine,[2-10] on the basis of the one-resolvent method and a simple diagrammatic representation. However, only some work on the two-resolvent method for Van Hove's original theory has been done.[11-13] One of the main reasons for such slow progress in the two-resolvent method is that the perturbation series of this theory has a much more complicated structure than does that of the one-resolvent method, and it does not have as simple a diagrammatic representation as does the one-resolvent method.

[1] Department of Physics, Tokyo Gakugei University, Koganei-shi, Tokyo, Japan.
[2] Department of Physics, Science University of Tokyo, Kagurazaka, Shinjuku-ku, Tokyo, Japan.

0022-4715/79/1000-0347$03.00/0

The first aim of the present work is to enhance the usefulness of the two-resolvent method by introducing a diagrammatic representation that gives for the perturbation series of this theory a parallel form to that for the one-resolvent method. Our idea involves the use of a superspace, which was introduced in our previous work.[13] According to the reformulation of this theory in the superspace, a diagrammatic representation called the product representation can be introduced. By using this representation, we can express the perturbation series in a form separated into four fundamental components: a creation part, a diagonal part, a destruction part, and a part representing the propagation of correlations, as in the one-resolvent method.[3] This product representation is further developed into an ordered product representation, which offers a very simple relationship between the asymptotic time dependence of each term in the perturbation series and the topological structure of the corresponding diagram. The collision kernel of the asymptotic kinetic equation can be systematically constructed from a compensative relation based on the conservation law of the probability.

The second aim of this work is to give a new treatment of quantum statistical effects in the asymptotic time evolution of a system on the basis of a systematic rule for the moving contraction technique,[14] and to show how the two-resolvent method is suitable for dealing with these complicated statistical effects. In our formalism, these effects are treated by noticing that some of the Fourier components of the Wigner distribution function are contracted to lower components through the symmetric properties of the wave function. In order to represent these effects of the contraction in a visualizable form, our diagrammatic method is further extended. We find that quantum statistical effects can be classified into two groups: internal ones among the particles in a collision, and external ones between a particle in a collision and a background particle. Consequently, by starting with a simple diagram in the Boltzmann statistics, we can include quantum statistical effects in our formalism merely by putting the two effects of the contraction into the original diagram.

We find that the collision kernels of the quantum statistical kinetic equations for various systems (examples treated are of a homogeneous system and of a linearized hydrodynamic system) can be easily obtained on the basis of the perturbation theory of the two-resolvent method.

2. FORMALISM

2.1. Introduction

As usual, we consider N identical particles with the Hamiltonian

$$H = H_0 + \lambda V = \sum_{i=1}^{N} \frac{\mathbf{p}_i^2}{2m} + \lambda \sum_{i<j}^{N} V(|\mathbf{r}_i - \mathbf{r}_j|) \tag{2.1}$$

in a cube of volume $(2\pi)^3\Omega$ with periodic boundary conditions, and introduce the unsymmetrized N-particle eigenstate of H_0, $|\mathbf{p}^N\rangle$, belonging to the eigenvalue $E_{\mathbf{p}^N} \equiv \sum_i^N \mathbf{p}_i^2/2m$, by

$$H_0|\mathbf{p}^N\rangle = E_{\mathbf{p}^N}|\mathbf{p}^N\rangle \tag{2.2}$$

which forms a complete orthonormal basis of the ordinary Hilbert space $\mathfrak{H}$, i.e.,

$$\langle\mathbf{p}^N|\mathbf{p}'^N\rangle = \prod_{i=1}^{N} \delta^{\mathrm{K}}(\mathbf{p}_i - \mathbf{p}_i') \tag{2.3}$$

$$\sum_{\mathbf{p}^N} |\mathbf{p}^N\rangle\langle\mathbf{p}^N| = 1 \tag{2.4}$$

Here, $\delta^{\mathrm{K}}(\mathbf{p})$ is the Kronecker symbol and the abbreviated notations $\mathbf{p}^N \equiv (\mathbf{p}_1,\ldots,\mathbf{p}_N)$ and $\sum_{\mathbf{p}^N} \equiv \sum_{\mathbf{p}_1}\cdots\sum_{\mathbf{p}_N}$ are used. The matrix element of the potential is given by

$$\langle\mathbf{p}^N|V|\mathbf{p}'^N\rangle = \Omega^{-1}\sum_{i<j}^{N}\sum_{\mathbf{q}} v(q)\,\delta^{\mathrm{K}}(\mathbf{p}_i - \mathbf{p}_i' + \hbar\mathbf{q})\,\delta^{\mathrm{K}}(\mathbf{p}_j - \mathbf{p}_j' - \hbar\mathbf{q}) \times \prod_{l\neq i,j}^{N} \delta^{\mathrm{K}}(\mathbf{p}_l - \mathbf{p}_l') \tag{2.5}$$

where $v(q)$ is the Fourier transform of $V(r)$, i.e.,

$$v(q) = \frac{1}{(2\pi)^3}\int d\mathbf{r}\, V(r)\exp(i\mathbf{q}r) \tag{2.6}$$

We are interested in an asymptotic system in the "thermodynamic limit" (T-limit), i.e.,

$$N\to\infty, \qquad \Omega\to\infty, \qquad N/\Omega = (2\pi)^3 c = \text{const} \tag{2.7}$$

where c is the density of the system. In the limit $\Omega\to\infty$, the Kronecker symbol and the summations on momentum and on wave vector are replaced by the Dirac delta function and integral signs, respectively, as

$$\hbar^3\Omega\,\delta^{\mathrm{K}}(\mathbf{p})\to\delta(\mathbf{p}), \qquad \hbar^3\Omega^{-1}\sum_{\mathbf{p}}\to\int d\mathbf{p}, \qquad \Omega^{-1}\sum_{\mathbf{q}}\to\int d\mathbf{q} \tag{2.8}$$

The symmetrized and antisymmetrized N-particle momentum states $|\mathbf{p}^N\rangle^{\mathrm{s}}$ are used as follows; from the basic states of (2.2) we have

$$|\mathbf{p}^N\rangle^{\mathrm{s}} \equiv (N!)^{1/2}\mathscr{S}_N|\mathbf{p}_1,\ldots,\mathbf{p}_N\rangle \tag{2.9}$$

where the symmetrization operator is defined in terms of the permutation operator Q, which replaces $\mathbf{p}_1$ by $\mathbf{p}_{Q_1},\ldots$ and $\mathbf{p}_N$ by $\mathbf{p}_{Q_N}$, by

$$\mathscr{S}_N = (1/N!)\sum_{Q}\theta^{n_Q}Q \tag{2.10}$$

Here, the sum on Q runs over the $N!$ permutations. The statistical factor θ is equal to 1 for bosons and -1 for fermions, and n_Q is the number of interchanges in a permutation Q. We further use the interchange operator Q_{ij}, which corresponds to the interchange of $\mathbf{p}_i$ and $\mathbf{p}_j$.

We now briefly explain our superspace $\mathfrak{S}$, which is a kind of unitary space consisting of linear operators $\{X, Y, \ldots\}$ in the Hilbert space $\mathfrak{H}$ (see Ref. 13 for more details). We denote the elements of the superspace by curly ket vectors $\{|X), |Y), \ldots\}$ and their adjoints by bra vectors $\{(X|, (Y|, \ldots\}$ and call them supervectors (s.vectors) or superstates (s.states). The inner product between them is defined by

$$(X|Y) = \mathrm{tr}[X^\dagger Y] = (Y^\dagger|X^\dagger) \tag{2.11}$$

where tr means the trace and $X^\dagger$ is the adjoint operator of X in $\mathfrak{H}$. We further introduce the "ordered superoperator," which is a kind of operator on $\mathfrak{S}$, as follows: Corresponding to two operators A and B in $\mathfrak{H}$, the ordered s.operator $(A \wedge B)$ is defined as

$$(A \wedge B)|Y) = |AYB) \tag{2.12}$$

for any s.vector $|Y)$. From this definition we get the formula for the product,

$$(A \wedge B)(C \wedge D) = (AC \wedge DB) \tag{2.13}$$

For brevity, it is convenient to introduce the "one-sided s.operators," which are defined by

$$A^> = (A \wedge 1), \qquad B^< = (1 \wedge B) \tag{2.14}$$

They satisfy the following relations:

$$(A \wedge B) = A^> B^< = B^< A^>, \quad (AB)^> = A^> B^>, \quad (AB)^< = B^< A^< \tag{2.15}$$

We further denote a dyad operator, $|\mathbf{p}^N\rangle\langle\mathbf{p}'^N|$ by a s.vector $|\mathbf{p}^N; \mathbf{p}'^N)$, which satisfies the eigenvalue equations

$$H_0{}^> |\mathbf{p}^N; \mathbf{p}'^N) = E_{\mathbf{p}^N} |\mathbf{p}^N; \mathbf{p}'^N), \qquad H_0{}^< |\mathbf{p}^N; \mathbf{p}'^N) = E_{\mathbf{p}'^N} |\mathbf{p}^N; \mathbf{p}'^N) \tag{2.16}$$

and forms a complete orthonormal basic set in $\mathfrak{S}$, i.e.,

$$(\mathbf{p}^N; \mathbf{p}'^N|\mathbf{q}^N; \mathbf{q}'^N) = \prod_{i=1}^{N} \prod_{j=1}^{N} \delta^{\mathrm{K}}(\mathbf{p}_i - \mathbf{q}_i)\, \delta^{\mathrm{K}}(\mathbf{p}_j' - \mathbf{q}_j') \tag{2.17}$$

$$\sum_{\mathbf{p}^N} \sum_{\mathbf{p}'^N} |\mathbf{p}^N; \mathbf{p}'^N)(\mathbf{p}^N; \mathbf{p}'^N| = 1 \tag{2.18}$$

A symmetrized dyad operator $|\mathbf{p}^N\rangle^{\mathrm{s}}{}^{\mathrm{s}}\langle\mathbf{p}'^N|$ is also denoted by $|\mathbf{p}^N; \mathbf{p}'^N)^{\mathrm{s}}$.

The density matrix $\rho(t)$ is expressed by a s.state $|\rho(t))$ in $\mathfrak{S}$ and is governed by the von Neumann equation,

$$i\hbar\, \partial_t |\rho(t)) = \mathscr{H} |\rho(t)) \tag{2.19}$$

where the antisymmetrized super-Hamiltonian $\tilde{\mathscr{H}}$ (the so-called super-Liouvillian) is defined by

$$\tilde{\mathscr{H}} \equiv H^{>} - H^{<} \tag{2.20}$$

Let us introduce the Wigner distribution function[3]

$$F_N(\mathbf{x}_1,\ldots,\mathbf{x}_N,\mathbf{p}_1,\ldots,\mathbf{p}_N,t) = \frac{1}{(2\pi\hbar)^3 N!}\sum_{\mathbf{k}^N}\exp\left[i\sum_{i=1}^{N}\mathbf{k}_i\mathbf{x}_i\right] \times {}^{s}\left(\mathbf{p}_1+\frac{\hbar}{2}\mathbf{k}_1,\ldots,\mathbf{p}_N+\frac{\hbar}{2}\mathbf{k}_N;\mathbf{p}_1-\frac{\hbar}{2}\mathbf{k}_1,\ldots,\mathbf{p}_N-\frac{\hbar}{2}\mathbf{k}_N|\rho(t)\right) \tag{2.21}$$

which is a useful tool for treating in a unified way a homogeneous and/or an inhomogeneous quantum system. The sets $\{\mathbf{x}_1,\ldots,\mathbf{x}_N\}$ and $\{\mathbf{p}_1,\ldots,\mathbf{p}_N\}$ are variables in the quantum phase space, where $\mathbf{x}_i$ is defined as a conjugate variable to the relative wave vector $\mathbf{k}_i$ of the ith momentum $\mathbf{p}_i \pm (\hbar/2)\mathbf{k}_i$ in the Fourier transform.

We assume that the Wigner distribution function is normalized in the T-limit as

$$\int (d\mathbf{x})^N \int (d\mathbf{p})^N F_N(\mathbf{x}^N,\mathbf{p}^N,0) = 1 \tag{2.22}$$

which corresponds to tr $\rho(0) = 1$ in $\mathfrak{H}$.

We further use the reduced distribution functions for a set of a finite number of particles, which are defined by

$$\begin{aligned} f_s(\mathbf{x}_1,\ldots,\mathbf{x}_s,\mathbf{p}_1,\ldots,\mathbf{p}_s,t) &= \frac{N!}{(N-s)!}\int (d\mathbf{x})^{N-s}\int (d\mathbf{p})^{N-s}F_N(\mathbf{x}^N,\mathbf{p}^N,t) \\ \phi_s(\mathbf{p}_1,\ldots,\mathbf{p}_s,t) &= \int (d\mathbf{x})^N\int (d\mathbf{p})^{N-s}F_N(\mathbf{x}^N,\mathbf{p}^N,t) \end{aligned} \tag{2.23}$$

A reduced description of the system is only meaningful in the case where the reduced Wigner functions exist in the T-limit. Then, following Prigogine and Balescu,[2] we introduce a Fourier component $\rho_{\mathbf{k}_1,\ldots,\mathbf{k}_r}$ for the Wigner function F_N as

$$\begin{aligned} F_N = (8\pi^3\Omega)^N\Big\{&\rho_0(|\ldots;t) + \Omega^{-1}\sum_{i}^{N}\sum_{\mathbf{k}_i}{}'\rho_{\mathbf{k}_i}(\mathbf{p}_i|\ldots;t)\exp(i\mathbf{k}_i\mathbf{x}_i) \\ &+ \Omega^{-2}\sum_{i<j}^{N}\sum_{\mathbf{k}_i}{}'\sum_{\mathbf{k}_j}{}'[\rho_{\mathbf{k}_i,\mathbf{k}_j}(\mathbf{p}_i,\mathbf{p}_j|\ldots;t) + \Omega\,\delta^{\mathrm{K}}(\mathbf{k}_i+\mathbf{k}_j) \\ &\times \rho_{\mathbf{k}_i,\mathbf{k}_j}(\mathbf{p}_i,\mathbf{p}_j|\ldots;t)]\exp[i(\mathbf{k}_i\mathbf{x}_i+\mathbf{k}_j\mathbf{x}_j)] + \cdots\Big\} \end{aligned} \tag{2.24}$$

and thus we get

$$\rho_{\mathbf{k}_1,\ldots,\mathbf{k}_r}(\mathbf{p}_1,\ldots,\mathbf{p}_r|\mathbf{p}_{r+1},\ldots,\mathbf{p}_N;t)$$

$$= \Omega^{N+\nu_r}(\hbar^{3N}N!)^{-1}$$

$$\times {}^{s}\Bigg(\mathbf{p}_1+\frac{\hbar}{2}\mathbf{k}_1,\ldots,\mathbf{p}_r+\frac{\hbar}{2}\mathbf{k}_r,\mathbf{p}_{r+1},\ldots,\mathbf{p}_N;\mathbf{p}_1-\frac{\hbar}{2}\mathbf{k}_1,\ldots,$$

$$\mathbf{p}_r-\frac{\hbar}{2}\mathbf{k}_r,\mathbf{p}_{r+1},\ldots,\mathbf{p}_N|\rho(t)\Bigg) \quad (2.25)$$

where the prime on the summation sign indicates the exclusion of $\mathbf{k}=0$, and ν_r is the number of independent nonzero wave vectors in $\mathbf{k}_1,\ldots\mathbf{k}_r$. In this component, the momentum argument on the left side of the bar indicates the center of momenta on the off-diagonal elements having nonzero relative momentum $\hbar\mathbf{k}$. For the case of a homogeneous system, only the components with $\sum_i \mathbf{k}_i = 0$ give a nonvanishing contribution for F_N. The component having all zero wave vectors, $\rho_0(\mathbf{p}^N;t)$, is simply the momentum distribution function, i.e., $\rho_0=\phi_N$. It is further assumed that the following factorization properties of the Fourier components hold[3,4]:

$$\rho_0(|\mathbf{p}_1,\ldots,\mathbf{p}_N;t)=\prod_{i=1}^{N}\phi_1(\mathbf{p}_i;t) \quad (2.26)$$

$$\rho_{\mathbf{k}_1,\ldots,\mathbf{k}_r}(\mathbf{p}_1,\ldots,\mathbf{p}_r|\mathbf{p}_{r+1},\ldots,\mathbf{p}_N;t)$$

$$=\rho^{(r)}_{\mathbf{k}_1,\ldots,\mathbf{k}_r}(\mathbf{p}_1,\ldots,\mathbf{p}_r;t)\prod_{i=r+1}^{N}\phi_1(\mathbf{p}_i;t) \quad (2.27)$$

Here, the reduced Fourier component is defined by

$$\rho^{(r)}_{\mathbf{k}_1,\ldots,\mathbf{k}_r}(\mathbf{p}_1,\ldots,\mathbf{p}_r;t)$$

$$=(\hbar^3\Omega^{-1})^{N-r}\sum_{\mathbf{p}_{r+1}}\cdots\sum_{\mathbf{p}_N}\rho_{\mathbf{k}_1,\ldots,\mathbf{k}_r}(\mathbf{p}_1,\ldots,\mathbf{p}_r|\mathbf{p}_{r+1},\ldots,\mathbf{p}_N;t) \quad (2.28)$$

and is closely related to the correlation function for the homogeneous system. Thus, the components having nonzero wave vectors are called "correlation components," and ρ_0 is the "vacuum component" for the homogeneous system.[3] The concepts of correlation component and vacuum component for inhomogeneous systems are extended in Sections 5 and 6.

2.2 Perturbations and Diagrams

The solution of the von Neumann equation (2.19) can be expressed by

$$|\rho(t)) = \mathscr{U}(t)|\rho(0)) \tag{2.29}$$

where the time evolution s.operator $\mathscr{U}(t)$ is defined by

$$\begin{aligned}\mathscr{U}(t) &= \exp(-i\mathscr{H}t/\hbar) \\ &= \left(\frac{-1}{2\pi i}\right)^2 \int_\Gamma dz \int_{\Gamma'} dz' \{\exp[-i(z-z')t/\hbar]\} R^>(z) R^<(z')\end{aligned} \tag{2.30}$$

Here, the resolvent s.operators are defined by $R^{\gtrless}(z) = (H^{\gtrless} - z)^{-1}$ and the paths of integration Γ and Γ' are any positive contours enclosing sufficiently large portions of the real axes in the complex z and z' planes, respectively (hereafter, for the symbols $>$ or $<$, the same symbols always have to be taken together).

The resolvents $R^{\gtrless}(z)$ satisfy the integral equation

$$R^{\gtrless}(z) = R_0{}^{\gtrless}(z) - \lambda R_0{}^{\gtrless}(z) V^{\gtrless} R^{\gtrless}(z) \tag{2.31}$$

with the unperturbed resolvents $R_0{}^{\gtrless}(z) = (H_0{}^{\gtrless} - z)^{-1}$; its iterated solution is

$$R^{\gtrless}(z) = R_0{}^{\gtrless}(z) \sum_{n=0}^{\infty} [-\lambda V^{\gtrless} R_0{}^{\gtrless}(z)]^n \tag{2.32}$$

Combining the above relations with (2.25), we obtain the perturbed solution for the Fourier component,

$$\begin{aligned}\rho_{\mathbf{k}^r}(\mathbf{p}^r|\mathbf{p}^{N-r}; t) = \left(\frac{-1}{2\pi i}\right)^2 \int_\Gamma dz \int_{\Gamma'} dz'\, e^{-i(z-z')t/\hbar} \\ \times \sum_{s=0}^{N} \Omega^{\nu_r - \nu_s} \sum_{i<j<\cdots}^{N} \sum_{\mathbf{p}'^N} \sum_{\mathbf{k}'^s}{}' \sum_{m=0}^{\infty} \sum_{n=0}^{\infty} \left(\left\{\mathbf{p} + \frac{\hbar}{2}\mathbf{k}\right\}^r, \mathbf{p}^{N-r};\right. \\ \left.\left\{\mathbf{p} - \frac{\hbar}{2}\mathbf{k}\right\}^r, \mathbf{p}^{N-r}|\{R_0(z)[-\lambda V R_0(z)]^m\right. \\ \wedge\ [-\lambda R_0(z') V]^n R_0(z')\}|\left\{\mathbf{p}' + \frac{\hbar}{2}\mathbf{k}'\right\}^s, \mathbf{p}'^{N-s};\right. \\ \left.\left\{\mathbf{p}' - \frac{\hbar}{2}\mathbf{k}'\right\}^s, \mathbf{p}'^{N-s}\right) \rho_{\mathbf{k}'^s}(\mathbf{p}'^s|\mathbf{p}'^{N-s}; 0)\end{aligned} \tag{2.33}$$

where $\{\mathbf{p} + \frac{1}{2}\hbar\mathbf{k}\}^r = \{\mathbf{p}_1 + \frac{1}{2}\hbar\mathbf{k}_1, \ldots, \mathbf{p}_r + \frac{1}{2}\hbar\mathbf{k}_r\}$ is used, and ν_r and ν_s are the numbers of independent nonzero wave vectors in $\rho_{\mathbf{k}^r}$ and $\rho_{\mathbf{k}'^s}$, respectively. The summations on $i, j, \ldots$ are taken over particles appearing in the initial Fourier component with nonzero wave vectors, except for particles appearing in the final component with nonzero wave vectors [see, for example, (2.35)]. In obtaining (2.33), we have used the symmetric property of the potential, $\mathscr{S}_N V = V\mathscr{S}_N$. Further, we have assumed, for the moment, that all intermediate states are summed independent of the other state and we have disregarded the special role of the diagonal transition, which is defined as a transition between states having the same momentum. Indeed, for such a case, we can see that each intermediate state gives the same contribution to the perturbation series irrespective of whether the state is symmetrized or not, and all quantum statistical effects may be crowded into the initial Fourier component as in (2.33). This neglect, of course, cannot be admitted in treating a large quantum system, and therefore we must recover our formalism later. However, in order to make our theory clear, here and in the next section we proceed by disregarding this effect, and we devote our attention only to the evolution part of (2.33). The details of how the quantum statistical effect is included in our theory are given in Section 4.

Let us introduce a diagram technique to analyze the behavior of this evolution part. In our diagram the tetradic element of an ordered s.operator

$$(\mathbf{p}^N; \mathbf{p}'^N|(A \wedge B)|\mathbf{q}^N; \mathbf{q}'^N) = \langle \mathbf{p}^N|A|\mathbf{q}^N\rangle\langle \mathbf{q}'^N|B|\mathbf{p}'^N\rangle \tag{2.34}$$

is represented by

$$\langle \mathbf{p}^N|A|\mathbf{q}^N\rangle|\langle \mathbf{q}'^N|B|\mathbf{p}'^N\rangle$$

where a vertical line between the matrix elements represents the symbol $\wedge$ at the corresponding location in the tetradic element and is called the Λ line. In the matrix elements, a momentum state for each particle is represented by a horizontal line to each side of the Λ line (see Fig. 1). On each line, the momentum and/or the name of the particle are put, if necessary. A potential is represented by a wavy vertical line and we put the momentum transfer on this line. In our diagram, a s.state is represented by a pair of states at either side of the Λ line, and a pair further from the Λ line corresponds to a s.-state further to the left in the term. To distinguish the vacuum part in the final s.state from its correlation part in which the particles have nonzero wave vectors, we draw nothing for particles having no wave vectors in the final s.state, and also for particles that appear in the intermediate or the initial s.state having the same momentum as the final ones (see Figs. 1 and 2a).

But, if necessary, we draw dotted horizontal lines for them, and call them vacuum lines. For instance, the contribution

$$
\begin{aligned}
&\rho_{\mathbf{k}_1}(\mathbf{p}_1|\mathbf{p}^{N-1};t) \\
&= \left(\frac{-1}{2\pi i}\right)^2 \int_\Gamma dz \int_{\Gamma'} dz'\, e^{-i(z-z')t/\hbar}(-\lambda)^2\Omega^{-1} \sum_i^N \sum_{\mathbf{p}'^{N-2}} \sum_{\mathbf{q}} \\
&\quad \times \Big(\mathbf{p}_1 + \frac{\hbar}{2}\mathbf{k}_1, \mathbf{p}^{N-1}; \mathbf{p}_1 - \frac{\hbar}{2}\mathbf{k}_1, \mathbf{p}^{N-1}|[R_0(z)VR_0(z) \wedge R_0(z')VR_0(z')] \\
&\quad \times |\mathbf{p}_1 + \frac{\hbar}{2}\mathbf{k}_1 + \hbar\mathbf{q}, \mathbf{p}_i, \mathbf{p}'^{N-2}; \mathbf{p}_1 - \frac{\hbar}{2}\mathbf{k}_1, \mathbf{p}_i + \hbar\mathbf{q}, \mathbf{p}'^{N-2}\Big) \\
&\quad \times \rho_{\mathbf{k}_1+\mathbf{q},-\mathbf{q}}\Big(\mathbf{p}_1 + \frac{\hbar}{2}\mathbf{q}, \mathbf{p}_i + \frac{\hbar}{2}\mathbf{q}|\mathbf{p}_j - \hbar\mathbf{q}, \mathbf{p}'^{N-3}; 0\Big) \\
&= \left(\frac{-1}{2\pi i}\right)^2 \int_\Gamma dz \int_{\Gamma'} dz'\, e^{-i(z-z')t/\hbar}(-\lambda)^2\Omega^{-1} \sum_{i<j}^N \Omega^{-2} \\
&\quad \times \sum_{\mathbf{q}} \frac{1}{E_{\mathbf{p}_1+(1/2)\hbar\mathbf{k}_1,\mathbf{p}_i,\mathbf{p}_j} - z} v(q) \frac{1}{E_{\mathbf{p}_1+(1/2)\hbar\mathbf{k}_1-\hbar\mathbf{q},\mathbf{p}_i,\mathbf{p}_j-\hbar\mathbf{q}} - z} \\
&\quad \times \frac{1}{E_{\mathbf{p}_1-(1/2)\hbar\mathbf{k}_1,\mathbf{p}_i+\hbar\mathbf{q},\mathbf{p}_j-\hbar\mathbf{q}} - z'} v(q) \frac{1}{E_{\mathbf{p}_1-(1/2)\hbar\mathbf{k}_1,\mathbf{p}_i,\mathbf{p}_j} - z'} \\
&\quad \times \rho_{\mathbf{k}_1+\mathbf{q},-\mathbf{q}}\Big(\mathbf{p}_1 + \frac{\hbar}{2}\mathbf{q}, \mathbf{p}_i + \frac{\hbar}{2}\mathbf{q}|\mathbf{p}_j - \hbar\mathbf{q}, \mathbf{p}^{N-3}; 0\Big) \qquad (2.35)
\end{aligned}
$$

is represented by the diagram shown in Fig. 1, and here we use an abbreviated notation for energies in which irrelevant arguments $\mathbf{p}^{N-3}$ are omitted for simplicity. In the diagram the symbol $\|$ on the initial particle line indicates that it is not diagonal at the time $t = 0$ and has nonzero wave vector corre-

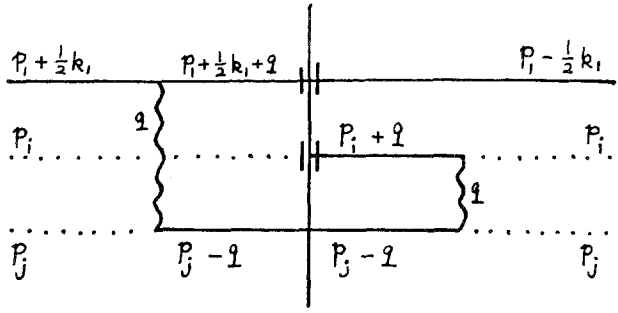

Fig. 1. Diagram corresponding to (2.35). We use units with $\hbar = 1$ in the diagram.

sponding to the initial correlation. These lines are called initially "excited" lines.

3. TIME EVOLUTION AND ORDERED PRODUCT REPRESENTATION

3.1. Time Dependence

We now develop our diagrammatic technique in order to discuss the time dependence of the perturbation series for a homogeneous system based on a classification of characteristic times, the relaxation time t_r and the collision time t_c, under the condition $t_r \gg t_c$. Our development is achieved in two steps: the first is the "product representation" (p.representation) and the second is the "ordered product representation" (o.p.representation).

To explain the p. representation, we first reformulate the perturbation series into four fundamental components: a destruction part, a diagonal part, a creation part, and a propagation-of-correlations part. This reformulation was done in Ref. 13 and the resultant expressions are

$$(\alpha;\beta|R^{>}(z)R^{<}(z')|\gamma;\delta) = (\alpha;\beta|\{[\mathscr{P} + \mathscr{Q}\mathscr{C}(z,z')\mathscr{P}]R^{>}(z)R^{<}(z') \times [\mathscr{P} + \mathscr{P}\mathscr{D}(z,z')\mathscr{Q}] + \mathscr{Q}\mathscr{I}(z,z')\mathscr{Q}\}|\gamma;\delta) \tag{3.1}$$

with the diagonal part

$$(\alpha;\alpha|\mathscr{P}R^{>}(z)R^{<}(z')\mathscr{P}|\beta;\beta) = \left(\alpha;\alpha\left|\sum_{i=0}^{\infty} D^{>}(z)D^{<}(z')[\mathscr{W}(z,z')D^{>}(z)D^{<}(z')]^{i}\right|\beta;\beta\right) \tag{3.2}$$

Here, Greek letters are used to express the eigenstates of the unperturbed Hamiltonian H_0 in $\mathfrak{H}$ for simplicity and the projection s.operators $\mathscr{P}$ and $\mathscr{Q}$ defined by

$$\mathscr{P} = \sum_{\alpha} |\alpha;\alpha)(\alpha;\alpha|, \qquad \mathscr{Q} = 1 - \mathscr{P} \tag{3.3}$$

are used. They satisfy the relations

$$\mathscr{P}^2 = \mathscr{P}, \qquad \mathscr{P}\mathscr{Q} = \mathscr{Q}\mathscr{P} = 0, \qquad \mathscr{Q}^2 = \mathscr{Q} \tag{3.4}$$

The irreducible s.operators are introduced as follows; the diagonal fragment is defined by

$$\mathscr{W}(z,z') = \mathscr{P}\{N^{>}(z)N^{<}(z')\}_{\text{t.ti}}\mathscr{P} \tag{3.5}$$

the creation part by

$$\mathscr{Q}\mathscr{C}(z,z')\mathscr{P} = \mathscr{Q}[D^{>}(z)N^{>}(z) + D^{<}(z')N^{<}(z') + D^{>}(z)D^{<}(z')\{N^{>}(z)N^{<}(z')\}_{\text{t.ti}}]\mathscr{P} \tag{3.6}$$

the destruction part by

$$\mathscr{P}\mathscr{D}(z, z')\mathscr{Q} = \mathscr{P}[N^{>}(z)D^{>}(z) + N^{>}(z')D^{>}(z') + \{N^{>}(z)N^{<}(z')\}_{\text{t.ti}}D^{>}(z)D^{<}(z')]\mathscr{Q} \tag{3.7}$$

and the propagation-of-correlations part by

$$\mathscr{Q}\mathscr{I}(z, z')\mathscr{Q} = \mathscr{Q}D^{>}(z)D^{<}(z')[1 + N^{>}(z)D^{>}(z) + N^{<}(z')D^{<}(z') + \{N^{>}(z)N^{<}(z')\}_{\text{t.ti}}D^{>}(z)D^{<}(z')]\mathscr{Q} \tag{3.8}$$

In these definitions

$$\langle\alpha|D(z)|\beta\rangle = D_{\alpha}(z)\,\delta^{\mathrm{K}}_{\alpha,\beta} = \left\langle \alpha \middle| \sum_{i=0}^{\infty} R_0(z)[G(z)R_0(z)]^i \middle| \alpha \right\rangle \delta^{\mathrm{K}}_{\alpha,\beta} \tag{3.9}$$

$$\langle\alpha|G(z)|\beta\rangle = G_{\alpha}(z)\,\delta^{\mathrm{K}}_{\alpha,\beta} = \left\langle \alpha \middle| \left\{ \sum_{i=0}^{\infty} - \lambda V[-\lambda R_0(z)V]^i \right\}_{\text{o.ti}} \middle| \alpha \right\rangle \delta^{\mathrm{K}}_{\alpha,\beta} \tag{3.10}$$

$$\langle\alpha|N(z)|\beta\rangle = N_{\alpha\beta}(z)(1 - \delta^{\mathrm{K}}_{\alpha,\beta}) = \left\langle \alpha \middle| \left\{ \sum_{i=0}^{\infty} - \lambda V[-\lambda R_0(z)V]^i \right\}_{\text{o.ti}} \middle| \beta \right\rangle (1 - \delta^{\mathrm{K}}_{\alpha,\beta}) \tag{3.11}$$

and

$$(\alpha;\beta|\{N^{>}(z)N^{<}(z')\}_{\text{t.ti}}|\gamma;\delta) = \left\langle \alpha \middle| \left\{ \sum_{i=0}^{\infty} - \lambda V[-\lambda R_0(z)V]^i \middle| \gamma \right\rangle \right. \times \left\langle \delta \middle| \sum_{j=0}^{\infty} - \lambda V[-\lambda R_0(z)V]^j \right\}_{\text{t.ti}} \middle| \beta \right\rangle (1 - \delta^{\mathrm{K}}_{\alpha,\gamma})(1 - \delta^{\mathrm{K}}_{\beta,\delta}) \tag{3.12}$$

Here, the subscript o.ti stands for "one-sided topologically irreducible," which implies that the intermediate states should never be identical to the initial and final states $|\alpha\rangle$ and $|\beta\rangle$, while t.ti stands for "two-sided topologically irreducible," which implies that the intermediate states on opposite sides of the operator $|\gamma\rangle\langle\delta|$ should never be identical to each other or to $|\alpha\rangle$, $|\beta\rangle$, $|\gamma\rangle$, and $|\delta\rangle$.[3]

The p. representation is devised so as to represent directly the above classification by diagrams. This representation is defined such that a product of diagrams is expressed in accordance with the product of the s.operators (2.13) as

$$AC|DB = A|B * C|D \tag{3.13}$$

Namely, when we decompose a diagram into the product, we put the innermost fragment of the original diagram onto the rightmost side. Further, we require that each fragment in this product is represented by the same rule as

[3] We note that in Ref. 13 the s.operators $G^{\gtrless}(z)$, $N^{\gtrless}(z)$, and $\{N^{>}(z)N^{<}(z')\}_{\text{irr}}$ were defined through the diagonal s.operator $D^{\gtrless}(z)$ instead of $R_0{}^{\gtrless}(z)$. This is why we use the concept of "topologically irreducible" rather than "irreducible" in this paper.

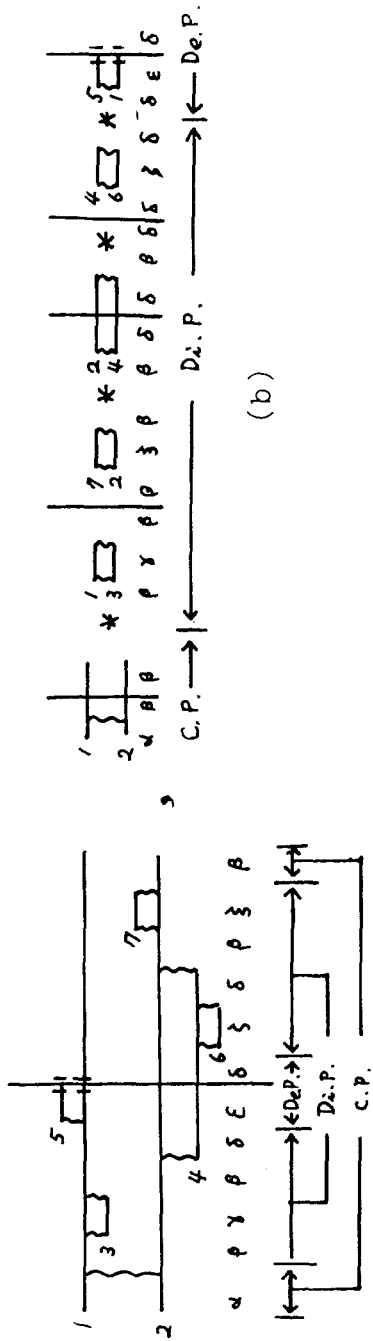

Fig. 2. Decomposition of a diagram into the product representation. C.P., creation part; Di.P., diagonal part; De.P., destruction part.

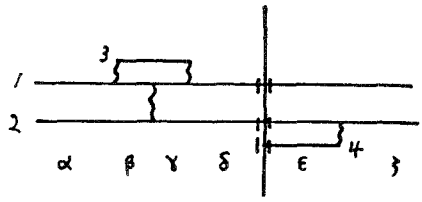

Fig. 3. Diagram representing the propagation-of-correlations.

for the original diagram; that is, we draw nothing for particles having no wave vectors in the final s.state of these fragments, and so on. An example is shown in Fig. 2, where the reducible diagram (a) is decomposed into the diagram (b). Under such a decomposition the fragments $G(z)$ and $\mathscr{W}(z, z')$ in the diagonal part can be separately represented in a simple form. We call the fragments G and $\mathscr{W}$ the "one-sided diagonal fragment" (o.s. diagonal fragment) and the "two-sided diagonal fragment" (t.s. diagonal fragment), respectively. We further use the terminology "diagonal s.state" or "vacuum s.state" in order to indicate the s.state having the same momentum states on opposite sides of the Λ line, such as $|\alpha; \alpha)$. For the propagation-of-correlations part we do not need to decompose into a product form. An example of this part is shown in Fig. 3.

As a result of this p. representation, the reconstructed perturbation series (3.1) can be represented in a visualizable form, and the diagonal part, which gives the main contribution in the asymptotic situation $t \gg t_c$, is detached from the other parts.

Let us now illustrate with the simple example of the diagonal part in Fig. 4 that this main contribution is given through the pole at $l = z - z' = 0$. The corresponding expression for $t > 0$ is

$$\rho_0(|\alpha; t)|_{\lambda^6} = \left(\frac{1}{2\pi i}\right)^2 \int_{-\infty}^{+\infty} dE \int_\gamma dl\, e^{-ilt/\hbar} \frac{1}{E_{\alpha_0} - E - \frac{1}{2}l} G^{(2)}_{\alpha_1}(E + \tfrac{1}{2}l)$$
$$\times \frac{1}{E_{\alpha_1} - E - \frac{1}{2}l} \frac{1}{E_{\alpha_{2'}} - E + \frac{1}{2}l} G^{(2)}_{\alpha_{2'}}(E - \tfrac{1}{2}l)$$
$$\times \frac{1}{E_{\alpha_{1'}} - E + \frac{1}{2}l} G^{(2)}_{\alpha_{1'}}(E - \tfrac{1}{2}l) \frac{1}{E_{\alpha_{0'}} - E + \frac{1}{2}l} \rho_0(|\alpha; 0) \quad (3.14)$$

where $\alpha_i = \alpha_j' = \alpha$, and $G^{(2)}_\alpha(z) = \lambda^2 \langle \alpha | \{V R_0(z) V\}_{\text{o.ti}} | \alpha \rangle$ is the lowest order term of λ in $G_\alpha(z)$ in (3.10), and we have changed the integration variables z

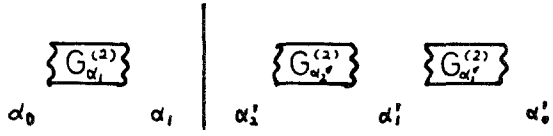

Fig. 4. Diagram corresponding to (3.14).

and z' to E and l. The path of the γ is parallel to the real axis on the upper half-plane of the complex l plane and goes to $-\infty$ from $+\infty$. The integrand in (3.14) has poles at $l = 0$ which come from the product of the propagators corresponding to the diagonal s.state, $(E_\alpha - E - \frac{1}{2}l)^{-2}(E_\alpha - E + \frac{1}{2}l)^{-3}$. These poles can be systematically exposed by the following procedure: We first decompose the factors on both sides of (3.14), $(E_{\alpha_0} - E - \frac{1}{2}l)^{-1}$ and $(E_{\alpha_0'} - E + \frac{1}{2}l)^{-1}$, into partial fractions. Then, we have the reduction formula

$$\begin{aligned}
&\frac{1}{E_{\alpha_0} - E - \frac{1}{2}l} G^{(2)}_{\alpha_1} \frac{1}{E_{\alpha_1} - E - \frac{1}{2}l} \frac{1}{E_{\alpha_2'} - E + \frac{1}{2}l} G^{(2)}_{\alpha_2'} \frac{1}{E_{\alpha_1'} - E + \frac{1}{2}l} \\
&\qquad \times G^{(2)}_{\alpha_1'} \frac{1}{E_{\alpha_0'} - E + \frac{1}{2}l} \\
&= \frac{1}{l} G^{(2)}_{\alpha_1'} \left[\frac{1}{E_{\alpha_0} - E - \frac{1}{2}l} G^{(2)}_{\alpha_1} \frac{1}{E_{\alpha_1} - E - \frac{1}{2}l} \frac{1}{E_{\alpha_1'} - E + \frac{1}{2}l} \right. \\
&\qquad \times G^{(2)}_{\alpha_2'} \frac{1}{E_{\alpha_1'} - E + \frac{1}{2}l} + \frac{1}{l}(-G^{(2)}_{\alpha_1}) \frac{1}{E_{\alpha_1} - E - \frac{1}{2}l} \frac{1}{E_{\alpha_2'} - E + \frac{1}{2}l} \\
&\qquad \left. \times G^{(2)}_{\alpha_2'} \frac{1}{E_{\alpha_1'} - E + \frac{1}{2}l} G^{(2)}_{\alpha_1'} \frac{1}{E_{\alpha_0'} - E + \frac{1}{2}l} \right] \qquad (3.15)
\end{aligned}$$

In the brackets in (3.15), we again decompose the factors on both sides into partial fractions. Continuing this procedure, we find the reduction of (3.14) as

$$\begin{aligned}
\rho_0(|\alpha; t)|_{\lambda^6} = \left(\frac{1}{2\pi i}\right)^2 \int_{-\infty}^{+\infty} dE \int_\gamma dl\, e^{-ilt/\hbar} \\
\times \left\{ \left[\frac{1}{l}(-G^{(2)}_{\alpha_1}) \frac{1}{l} G^{(2)}_{\alpha_1'} \frac{1}{l} G^{(2)}_{\alpha_2'} \frac{1}{l} + \frac{1}{l} G^{(2)}_{\alpha_1'} \frac{1}{l}(-G^{(2)}_{\alpha_1}) \frac{1}{l} G^{(2)}_{\alpha_2'} \frac{1}{l} \right. \right. \\
\left. + \frac{1}{l} G^{(2)}_{\alpha_1'} \frac{1}{l} G^{(2)}_{\alpha_2'} \frac{1}{l}(-G^{(2)}_{\alpha_1}) \frac{1}{l} \right] \frac{1}{E_{\alpha_1} - E - \frac{1}{2}l} + [\cdots](-1) \frac{1}{E_{\alpha_2'} - E + \frac{1}{2}l} \\
+ \left[\frac{1}{l} G^{(2)}_{\alpha_1'} \frac{1}{l} G^{(2)}_{\alpha_2'} \frac{1}{l} \right] \frac{1}{E_{\alpha_0} - E - \frac{1}{2}l} G^{(2)}_{\alpha_1} \frac{1}{E_{\alpha_1} - E - \frac{1}{2}l} \\
+ \left[\frac{1}{l}(-G^{(2)}_{\alpha_1}) \frac{1}{l} G^{(2)}_{\alpha_1'} \frac{1}{l} + \frac{1}{l} G^{(2)}_{\alpha_1'} \frac{1}{l}(-G^{(2)}_{\alpha_1}) \frac{1}{l} \right](-1) \\
\times \frac{1}{E_{\alpha_1'} - E + \frac{1}{2}l} G^{(2)}_{\alpha_2'} \frac{1}{E_{\alpha_2'} - E + \frac{1}{2}l} + \left[\frac{1}{l}(-G^{(2)}_{\alpha_1}) \frac{1}{l} \right](-1) \\
\left. \times \frac{1}{E_{\alpha_0'} - E + \frac{1}{2}l} G^{(2)}_{\alpha_1'} \frac{1}{E_{\alpha_1'} - E + \frac{1}{2}l} G^{(2)}_{\alpha_2'} \frac{1}{E_{\alpha_2'} - E + \frac{1}{2}l} \right\} \rho_0(|\alpha; 0) \\
(3.16)
\end{aligned}$$

The integrands in (3.16) have analytical continuations in the lower half-plane in l and the poles at $l = 0$ are sufficiently isolated for the case of short-range interactions. Thus, it is enough to consider the contributions of the poles at $l = 0$ for $t \gg t_c$, and we get, for example, for the first term in (3.16),

$$\rho_0(|\alpha; t)|_{\lambda^6 \text{f.t.}} = \frac{1}{2\pi i} \int_{-\infty}^{+\infty} dE \sum_{r=0}^{3} \frac{1}{(3-r)!} \left(\frac{-it}{\hbar}\right)^{3-r} \frac{\partial^r}{\partial l^r} \times [-G^{(2)}_{\alpha_1}(E + \tfrac{1}{2}l) G^{(2)}_{\alpha_1'}(E - \tfrac{1}{2}l) G^{(2)}_{\alpha_2'}(E - \tfrac{1}{2}l) + \cdots] \times \frac{1}{E_{\alpha_1} - E - \frac{1}{2}l} \Big|_{l=+i0} \rho_0(|\alpha; 0) \tag{3.17}$$

As shown by this example, the diagonal part gives the contribution that grows with time. Therefore, our separation of the diagram with the aid of the p. representation is useful for treating the asymptotic time behavior of the system. However, in this representation there is no unique correspondence between the number diagonal fragments and the orders of the poles at $l = 0$. So, in order to derive the generalized master equation through our diagrammatic method, some improvements are needed in the p. representation. We note that this disaccord is caused by the existence of an ambiguity in the order with regard to time between an o.s. diagonal fragment on the left-hand side and one on the right-hand side of the Λ line. Therefore, if these fragments are further rearranged in the p. representation by imposing an order between them, the disaccord can be resolved. This is the second step of our development and is achieved in the following subsection by introducing the ordered product representation.

3.2. Ordered Product Representation

We now explain the o.p. representation by using the same example. For this purpose, let us first note the order of the diagonal fragments in the reduction in (3.16). There, the arrangement of these fragments has been achieved in a regular form: In the first two brackets in (3.16), there appear all terms corresponding to the permutations between the fragments $-G^{(2)}_{\alpha_i}$ and $G^{(2)}_{\alpha_j'}$, which are on opposite sides of the Λ line (no permutations among the fragments on the same side of the Λ line appear, since there is already a definite order among them in the original diagram). There are other terms in (3.16) where some of the innermost fragments are incorporated into the propagators, such as $(E_{\alpha_0} - E - \frac{1}{2}l)^{-1} G^{(2)}_{\alpha_1}$ $(E_{\alpha_1} - E - \frac{1}{2}l)^{-1}$, or $-(E_{\alpha_1'} - E + \frac{1}{2}l)^{-1} G^{(2)}_{\alpha_2'} (E_{\alpha_2'} - E + \frac{1}{2}l)^{-1}$, rather than being arranged in an order similar to the above one, and they no longer play the role of a diagonal

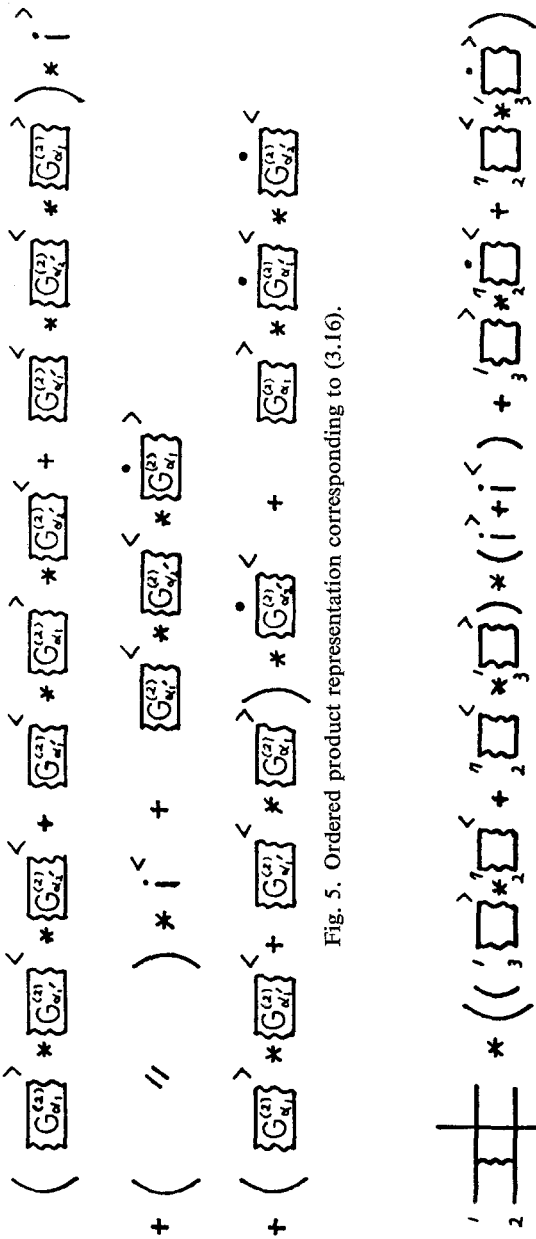

Fig. 5. Ordered product representation corresponding to (3.16).

Fig. 6. Ordered product representation for the diagram in Fig. 2b.

fragment contributing to the asymptotic time evolution, since they do not have the factor l^{-1}. These "inactivated" diagonal fragments yield part of the renormalized propagator in the perturbation theory.

In the more general situation, the rule with regard to this reduction also holds for an arbitrary number of o.s. diagonal fragments in a diagonal s.state. The details of the reduction are given in Appendix A.

The rule for the o.p. representation is as follows: The one-sided diagonal fragments in the same diagonal s.state are arranged in accordance with the order in (3.16) or (A2) as shown in Fig. 5. The symbol $>$ ($<$) on a fragment indicates that this fragment is located at the left- (right-) hand side of the Λ line in the original diagram. The dotted fragments are renormalized into the propagator and are inactivated in the time evolution. The symbols $\mathrm{i}^{>}$ and $\mathrm{i}^{<}$ represent the propagators $(E_\alpha - E - \frac{1}{2}l)^{-1}$ and $-(E_\alpha - E + \frac{1}{2}l)^{-1}$, respectively. Then, by using the o.p. representation, we can further decompose the diagram in Fig. 2b as shown in Fig. 6.

We remark here that if the reduction formula (A3) is used instead of (A2) for the decomposition of the original term, another o.p. representation is possible. In this case, however, the dotted fragment or $\mathrm{i}^{\gtrless}$ is located on the left-hand side in each diagonal s.state, in contrast with the above-mentioned o.p. representation. An example is shown in Fig. 7.

As a consequence of our diagrammatic method, we can state a very simple theorem concerning to the relationship between the number of diagonal fragments and the order of a pole at $l = 0$ in the o.p. representation:

Theorem. Any diagram consisting of m diagonal fragments except for the dotted fragments has a pole of $(m + 1)$th order at $l = 0$.

A simple application of this theorem is shown in Fig. 8, where all diagonal parts having simple poles at $l = 0$ are summed. The terms for these diagrams are expressed with the renormalized propagators $D_\alpha(E \pm \frac{1}{2}l)$ as

$$\begin{aligned}
&\frac{1}{l}\left[D_\alpha\left(E + \frac{1}{2}l\right) - D_\alpha\left(E - \frac{1}{2}l\right)\right] \\
&\quad = \frac{1}{l}\left\{\sum_{i=0}^{\infty} \frac{1}{E_\alpha - E - \frac{1}{2}l}\left[G_\alpha\left(E + \frac{1}{2}l\right)\frac{1}{E_\alpha - E - \frac{1}{2}l}\right]^i\right. \\
&\qquad \left. - \sum_{j=0}^{\infty} \frac{1}{E_\alpha - E + \frac{1}{2}l}\left[G_\alpha\left(E - \frac{1}{2}l\right)\frac{1}{E_\alpha - E + \frac{1}{2}l}\right]^j\right\} \\
&\quad = \frac{1}{l}\left[\frac{1}{E_\alpha - E - \frac{1}{2}l - G_\alpha(E + \frac{1}{2}l)} - \frac{1}{E_\alpha - E + \frac{1}{2}l - G_\alpha(E - \frac{1}{2}l)}\right]
\end{aligned} \tag{3.18}$$

In a similar way, we can obtain simple expressions for the summation of all diagonal parts as shown in Fig. 9, where Fig. 9a is obtained from the

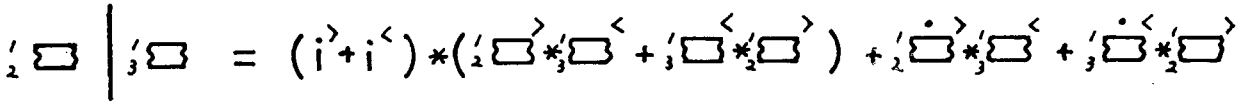

Fig. 7. Another type of ordered product representation.

Fig. 8. Summation of all diagonal parts having simple poles at $l = 0$.

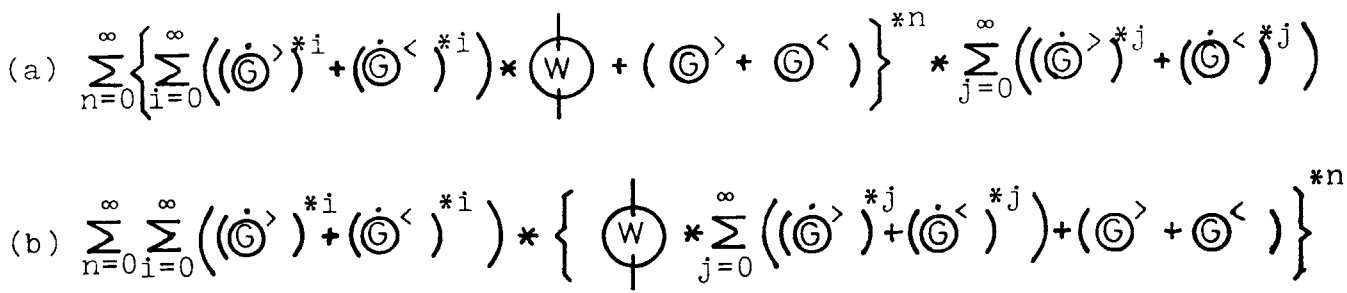

Fig. 9. Summations of all diagonal parts.

reduction formula (A2) and Fig. 9b is from (A3). The corresponding terms are expressed by the s.operators as

$$(\alpha;\alpha|\mathscr{P}R^{>}(E+\tfrac{1}{2}l)R^{<}(E-\tfrac{1}{2}l)\mathscr{P}|\beta;\beta)$$

$$=\sum_{n=0}^{\infty}(\alpha;\alpha|\left[\frac{1}{l}\chi_E(l)\right]^n\frac{1}{l}\Delta_E(l)|\beta;\beta) \tag{3.19a}$$

$$=\sum_{n=0}^{\infty}(\alpha;\alpha|\Delta_E(l)\frac{1}{l}\left[\tilde{\chi}_E(l)\frac{1}{l}\right]^n|\beta;\beta) \tag{3.19b}$$

where

$$\Delta_E(l)=\mathscr{P}[D^{>}(E+\tfrac{1}{2}l)-D^{<}(E-\tfrac{1}{2}l)]\mathscr{P} \tag{3.20}$$

$$\mathscr{G}_E(l)=\mathscr{P}[G^{>}(E+\tfrac{1}{2}l)-G^{<}(E-\tfrac{1}{2}l)]\mathscr{P} \tag{3.21}$$

$$\chi_E(l)=\Delta_E(l)\mathscr{W}(E+\tfrac{1}{2}l,E-\tfrac{1}{2}l)-\mathscr{G}_E(l) \tag{3.22}$$

$$\tilde{\chi}_E(l)=\mathscr{W}(E+\tfrac{1}{2}l,E-\tfrac{1}{2}l)\Delta_E(l)-\mathscr{G}_E(l) \tag{3.23}$$

The generalized master equation can be easily obtained by using the expressions in (3.19). For this purpose we first introduce a partial distribution function of momenta defined by

$$\rho_{0,E}(|\mathbf{p}^N;t)=\left(\frac{1}{2\pi i}\right)^2\int_\gamma dl\,e^{-ilt/\hbar}\sum_{m=0}^{\infty}\sum_{\mathbf{p}'^N}\left(\frac{1}{l}\right)^{m+1}$$
$$\times(\mathbf{p}^N;\mathbf{p}^N|\chi_E{}^m(l)\Delta_E(l)|\mathbf{p}'^N;\mathbf{p}'^N)[\rho_0(|\mathbf{p}^N;0)$$
$$+\sum_{s=1}^{N}\Omega^{-\nu_s}\sum_{1<j<\cdots<s}^{N}\sum_{\mathbf{p}''^N}\sum_{\mathbf{k}''^s}{}'(\mathbf{p}'^N;\mathbf{p}'^N|\mathscr{D}(E+\tfrac{1}{2}l,E-\tfrac{1}{2}l)$$
$$\times\left|\left\{\mathbf{p}''+\frac{\hbar}{2}\mathbf{k}''\right\}^s,\mathbf{p}''^{N-s};\left\{\mathbf{p}''-\frac{\hbar}{2}\mathbf{k}''\right\}^s,\mathbf{p}''^{N-s}\right)\rho_{\mathbf{k}''^s}(\mathbf{p}''^s|\mathbf{p}''^{N-s};0)] \tag{3.24}$$

For $t>0$, the relation

$$\rho_0(|\mathbf{p}^N;t)=\int_{-\infty}^{+\infty}dE\,\rho_{0,E}(|\mathbf{p}^N;t) \tag{3.25}$$

holds. By differentiating (3.24) with respect to t and by using the convolution theorem for the Laplace transform, we obtain the generalized master equation as

$$i\hbar\,\partial_t\rho_{0,E}(|\mathbf{p}^N;t)=h_E(\mathbf{p}^N;t)$$
$$+\frac{2\pi}{\hbar}\int_0^t d\tau\sum_{\mathbf{p}'^N}(\mathbf{p}^N;\mathbf{p}^N|\chi_E{}'(\tau)|\mathbf{p}'^N;\mathbf{p}'^N)\rho_{0,E}(|\mathbf{p}'^N;t-\tau) \tag{3.26}$$

where

$$h_E(\mathbf{p}^N; t) = \left(\frac{1}{2\pi i}\right)^2 \int_\gamma dl\, e^{-ilt/\hbar}(\mathbf{p}^N; \mathbf{p}^N|\Delta_E(l)|\mathbf{p}^N; \mathbf{p}^N)$$
$$\times \left[\rho_0(|\mathbf{p}^N; 0) + \sum_{s=1}^{N} \Omega^{-\nu_s} \sum_{i<j<\cdots<s}^{N} \sum_{\mathbf{p}'^N} \sum_{\mathbf{k}'s}{}' (\mathbf{p}^N; \mathbf{p}^N|\mathscr{D}(E + \tfrac{1}{2}l, E - \tfrac{1}{2}l)\right.$$
$$\left. \times \left|\left\{\mathbf{p}' + \frac{\hbar}{2}\mathbf{k}'\right\}^s, \mathbf{p}^{N-s}; \left\{\mathbf{p}'^N - \frac{\hbar}{2}\mathbf{k}'\right\}^s, \mathbf{p}^{N-s}\right)\rho_{\mathbf{k}'s}(\mathbf{p}'^s|\mathbf{p}'^{N-s}; 0)\right] \tag{3.27}$$

and

$$(\mathbf{p}^N; \mathbf{p}^N|\chi_E'(t)|\mathbf{p}'^N; \mathbf{p}'^N)$$
$$= \left(\frac{1}{2\pi i}\right)^2 \int_\gamma dl\, e^{-ilt/\hbar}(\mathbf{p}^N; \mathbf{p}^N|\chi_E(l)|\mathbf{p}'^N; \mathbf{p}'^N) \tag{3.28}$$

The s.operators χ and $\tilde{\chi}$ are called "collision s.operators" of the generalized master equation and are identical to (3.40) and (3.41) of Ref. 13. The s.operators $\Delta\mathscr{W}$ and $\mathscr{W}\Delta$ are the "gain parts" of the collision s.operators and $\mathscr{G}$ is the "loss part." We further note that if only the poles at $l = 0$ are evaluated in (3.24), the asymptotic generalized master equation is obtained as

$$i\hbar\, \partial_t \rho_{0,E}(|\mathbf{p}^N; t)$$
$$= \frac{2\pi}{\hbar} \int_0^\infty dt \sum_{\mathbf{p}'^N} (\mathbf{p}^N; \mathbf{p}^N|\chi_E'(\tau)|\mathbf{p}'^N; \mathbf{p}'^N)\rho_{0,E}(|\mathbf{p}'^N; t - \tau) \tag{3.29}$$

This equation is consistent with the equation for the asymptotic evolution s.operator $\Sigma_E^{(+)}(t)$ in (4.22) of Ref. 13. Equation (3.29) is derived in Appendix B.

3.3. Construction of the Collision S.operator and the Compensative Relation

We now refer to a useful relationship among diagrams which plays an essential role throughout our work on quantum statistical systems. In our diagrammatic method it seems that the t.s. fragment has a complicated structure as compared with the o.s. fragment. However, if we take note of a compensative relation between these fragments which ensures that the conservation law of the probability holds, i.e.,

$$1 = \sum_{\mathbf{p}^N} (\mathbf{p}^N; \mathbf{p}^N|\rho(0)) = \sum_{\mathbf{p}^N} (\mathbf{p}^N; \mathbf{p}^N|\mathscr{U}(t)|\rho(0)) \tag{3.30}$$

then we can unravel the complicated structure of the t.s. fragment through the study of the simple o.s. fragment.

To illustrate this, let us consider how the conservation law can hold in our perturbation theory. From (3.30) we see that in order to ensure that this law holds, there must be a cancellation among diagrams having the same initial and the same intermediate states with the same order of λ. These cancelating diagrams are called "compensative diagrams" and can be found by the following systematic rule: We first draw any o.s. diagram, such as the example in Fig. 10a. Next, the leftmost potential, together with the states on either side of it, is transferred to the furthermost opposite side, as in the diagram of Fig. 10b. The third diagram, Fig. 10c, is similarly obtained from the second by transferring the leftmost potential, and the successive transfers are continued until we obtain the diagram of Fig. 10f, in which all potentials are on the right-hand side of the Λ line. Then, we get all compensative diagrams from the original one. The cancellation of these diagrams can be seen in the following manner: In each term, decomposing only the outermost product of the propagator, such as $(E_\alpha - E - \frac{1}{2}l)^{-1}(E_\alpha - E + \frac{1}{2}l)^{-1}$ in Fig. 10a, into partial fractions, then we find that all terms cancel except for some parts of the partial fractions in Figs. 10a and 10f. Further, the uncanceled parts vanish themselves by the integration over E, since all their poles for E are located on the same side of the real axis.[4] Hence, we can confirm that due to the compensative relation, all terms except for the zeroth-order term in λ cancel under summations of all momenta and (3.30) holds.

Let us see the utility of the compensative relation in the construction of the collision s.operator. Since the compensative relation holds irrespective of l, the terms having the same order of l^{-1} in the compensative diagrams must cancel each other. Thus, in the o.p. representation, the diagrams in a collision s.operator must cancel. For example, the diagrams in Fig. 11, which are obtained from Fig. 10 as those proportional to l^{-2}, cancel each other.

On the other hand, if a reduced function is of interest, and, for example, if the momentum of the particle 1 in Fig. 11 is not summed as a fixed particle appearing in the reduced function, the compensative diagrams in the first and second brackets can survive into the gain and loss parts of the collision s.operator, respectively. Thus, our formalism leads to the ordinary type of collision kernel in the asymptotic equation, in which the gain and the loss parts are separately represented in a compensative form. This result is in contrast with the one obtained from the one-resolvent method,[3] where these parts are merged into a single collision kernel.

In applying this rule to constructing the collision s.operator, it is worthwhile noting that if we start with the o.s. diagonal fragment having an intermediate diagonal transition (this type of transition is called a "bubble" or

[4] We remark that if the integration over E is not performed, these parts contribute to the inhomogeneous term $h_E(t)$ of the generalized master equation (3.26).

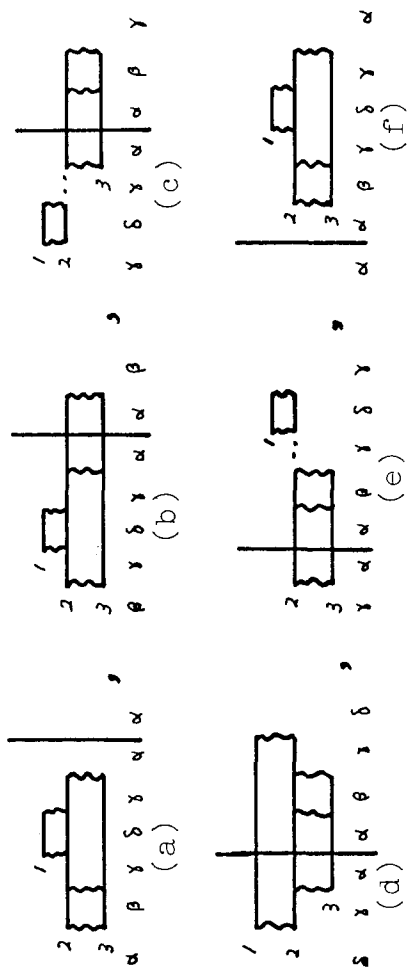

Fig. 10. Compensative diagrams.

Fig. 11. Compensative diagrams obtained from Fig. 10 as those proportional to I^{-2}.

"self-energy"), then in the t.s. diagram there appears an additional diagonal fragment corresponding to this bubble (see Fig. 10). Therefore, when we gather the compensative diagrams having the same order of l^{-1} in the o.p. representation, the original o.s. fragment having the bubble must be always paired with the t.s. fragment having the inactivated diagonal fragment corresponding to the bubble as shown in Fig. 11. On the other hand, the o.s. diagonal fragment having no bubble never yields any additional one in the t.s. diagram, and moreover, these o.s. and t.s. fragments have the form of the same topological type of diagram irrespective of the location of their Λ line. These types of fragments ("skeleton fragments") constitute the basic elements in our diagrammatic method, because any diagram can be built up merely by putting the bubbles on the propagators in these skeleton fragments. Moreover, this procedure is expressed by replacing the free propagators with the renormalized propagators D_α of (3.9).

The peculiar structure of a diagram having a bubble or inactivated diagonal fragment as compared with the skeleton fragment is that the former always has a singularity of higher order than the free propagator. This implies that this fragment may contribute to the time evolution only in such a situation that the collision time t_c cannot be neglected as compared with the relaxation time. Therefore, when we treat a system in which t_c may be considered as being instantaneous, it is enough to concern ourselves only with the skeleton fragments. This fact also supports the notion that the skeleton fragments form the basic frames of the two-resolvent method.

As a consequence of the above discussion, we can summarize our procedure for building up the collision s.operator as follows:

1. Draw an o.s. diagonal skeleton fragment.
2. Transfer successively the outermost potential originally on one side of the Λ line to the opposite outermost side until the opposite o.s. fragment is obtained.
3. Put the bubbles and/or the inactivated diagonal fragments onto each propagator in the skeleton fragments obtained in steps 1 and 2.

Then, we can obtain the diagrams for which we are looking.

We mention another use of the compensative relation; it concerns the concept of the connectedness in the diagram and leads to the restriction of the number of diagrams which we must treat. That is, if we are interested in the reduced properties of the system, it is enough to treat only the "connected diagram" containing the fixed particle, where by connected diagram we mean that the diagram consists of subgroups having a particle in common (see Fig. 12). This theorem can be proved by the aid of the convolution technique introduced by Hugenholtz.[15] To avoid digressing from our subject, we give the details in Appendix C.

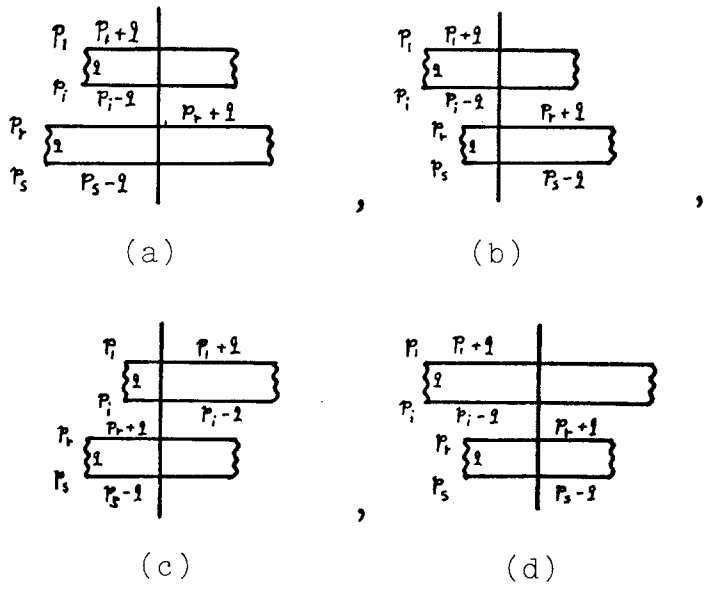

Fig. 12. Examples of "disconnected" diagrams consisting of two "connected" subgroups.

4. QUANTUM STATISTICAL EFFECT AND CONTRACTION

4.1. Contraction

We now show how the quantum statistical effect is treated in our formalism. We consider a simple example of a correlation component $\rho_{\mathbf{k}_i,\mathbf{k}_j}(\mathbf{p}_i, \mathbf{p}_j|\mathbf{p}^{N-2})$ with $\mathbf{k}_i + \mathbf{k}_j \neq 0$. From (2.25) the relation

$$\rho_{\mathbf{k}_i,\mathbf{k}_j}(\mathbf{p}_i, \mathbf{p}_j|\mathbf{p}^{N-2}) = \frac{\Omega^{N+2}\, s}{\hbar^3 N!}\left(\mathbf{p}_i + \frac{\hbar}{2}\mathbf{k}_i, \mathbf{p}_j + \frac{\hbar}{2}\mathbf{k}_j, \mathbf{p}^{N-2}; \mathbf{p}_i - \frac{\hbar}{2}\mathbf{k}_i, \mathbf{p}_j - \frac{\hbar}{2}\mathbf{k}_j, \mathbf{p}^{N-2}|\rho\right) \tag{4.1}$$

holds and it seems that this is an off-diagonal Fourier component having two nonzero wave vectors $\mathbf{k}_i$ and $\mathbf{k}_j$. However, due to the symmetric (or anti-symmetric) property of the momentum state, if $\mathbf{p}_i + (\hbar\mathbf{k}_i/2) = \mathbf{p}_j - (\hbar\mathbf{k}_j/2)$, then (4.1) reduces to a lower component having a single wave vector $\mathbf{k}_i + \mathbf{k}_j$ as

$$\theta\Omega\, \delta^{\mathrm{K}}\left(\mathbf{p}_i + \frac{\hbar}{2}\mathbf{k}_i - \mathbf{p}_j + \frac{\hbar}{2}\mathbf{k}_j\right)\rho_{\mathbf{k}_i+\mathbf{k}_j}\left(\mathbf{p}_i + \frac{\hbar}{2}\mathbf{k}_j|\mathbf{p}_j - \frac{\hbar}{2}\mathbf{k}_j, \mathbf{p}^{N-2}\right) \tag{4.2}$$

where the statistical factor θ comes from the interchange of the roles of the

particles i and j on the left-hand state in (4.1), and (2.25) is again used. Since the factor $\Omega\delta^{\mathrm{K}}$ in (4.2) exactly coincides with the δ-function in the T-limit, this δ-singular term cannot be neglected as compared with the nonsingular term in (4.1) for large quantum systems. This reduction is just the quantum statistical effect that originates from the symmetric property of the particles and is called a "contraction."[4,14]

Except for the components $\rho_0(|\mathbf{p}^N)$ and $\rho_{\mathbf{k}_j}(\mathbf{p}_j|\mathbf{p}^{N-1})$, contractions occur in any Fourier components and these contractions are performed as follows: First, the contraction between any two particles having nonzero wave vectors in $\rho_{\mathbf{k}^r}$ is performed by the following contraction formulas:

(i) For $\mathbf{k}_i + \mathbf{k}_j \neq 0$

$$\begin{aligned}
&\rho_{\mathbf{k}_i,\mathbf{k}_j,\mathbf{k}^{r-2}}(\mathbf{p}_i, \mathbf{p}_j, \mathbf{p}^{r-2}|\mathbf{p}^{N-r}) \\
&= \rho'_{\mathbf{k}_i,\mathbf{k}_j,\mathbf{k}^{r-2}}(\mathbf{p}_i, \mathbf{p}_j, \mathbf{p}^{r-2}|\mathbf{p}^{N-r}) \\
&\quad + \theta\Omega\,\delta^{\mathrm{K}}\left(\mathbf{p}_i + \frac{\hbar}{2}\mathbf{k}_i - \mathbf{p}_j + \frac{\hbar}{2}\mathbf{k}_j\right) \\
&\quad \times \rho_{\mathbf{k}_i+\mathbf{k}_j,\mathbf{k}^{r-2}}\left(\mathbf{p}_i + \frac{\hbar}{2}\mathbf{k}_j, \mathbf{p}^{r-2}\middle|\mathbf{p}_j - \frac{\hbar}{2}\mathbf{k}_j, \mathbf{p}^{N-r}\right) \\
&\quad + \theta\Omega\,\delta^{\mathrm{K}}\left(\mathbf{p}_i - \frac{\hbar}{2}\mathbf{k}_i - \mathbf{p}_j + \frac{\hbar}{2}\mathbf{k}_j\right) \\
&\quad \times \rho_{\mathbf{k}_i+\mathbf{k}_j,\mathbf{k}^{r-2}}\left(\mathbf{p}_j + \frac{\hbar}{2}\mathbf{k}_i, \mathbf{p}^{r-2}\middle|\mathbf{p}_i - \frac{\hbar}{2}\mathbf{k}_i, \mathbf{p}^{N-r}\right)
\end{aligned} \tag{4.3a}$$

(ii) For $\mathbf{k}_i + \mathbf{k}_j = 0$

$$\begin{aligned}
&\rho_{\mathbf{k}_i,-\mathbf{k}_i,\mathbf{k}^{r-2}}(\mathbf{p}_i, \mathbf{p}_j, \mathbf{p}^{r-2}|\mathbf{p}^{N-r}) \\
&\quad = \rho'_{\mathbf{k}_i,-\mathbf{k}_i,\mathbf{k}^{r-2}}(\mathbf{p}_i, \mathbf{p}_j, \mathbf{p}^{r-2}|\mathbf{p}^{N-r}) \\
&\qquad + \theta\Omega\,\delta^{\mathrm{K}}(\mathbf{p}_i - \mathbf{p}_j)\rho_{\mathbf{k}^{r-2}}\left(\mathbf{p}^{r-2}\middle|\mathbf{p}_i - \frac{\hbar}{2}\mathbf{k}_i, \mathbf{p}_j + \frac{\hbar}{2}\mathbf{k}_i, \mathbf{p}^{N-r}\right)
\end{aligned} \tag{4.3b}$$

Here, the primes on the $\rho_{\mathbf{k}^r}$ indicate that their singular parts at $\mathbf{p}_i \pm (\hbar\mathbf{k}_i/2) = \mathbf{p}_j \mp (\hbar\mathbf{k}_j/2)$ are removed. We apply these formulas successively to the remaining particles having nonzero wave vectors until all contractible parts are separated. Then, we can find the component $\rho_{\mathbf{k}^r}$ expressed in terms of nonsingular components $\tilde{\rho}_{\mathbf{k}^s}$ $(s \leqslant r)$, which are defined as components no longer having a contractible part in $\rho_{\mathbf{k}^s}$.

In order to perform this contracting procedure systematically, we develop our diagrammatic method as follows: We draw the contracted part of the

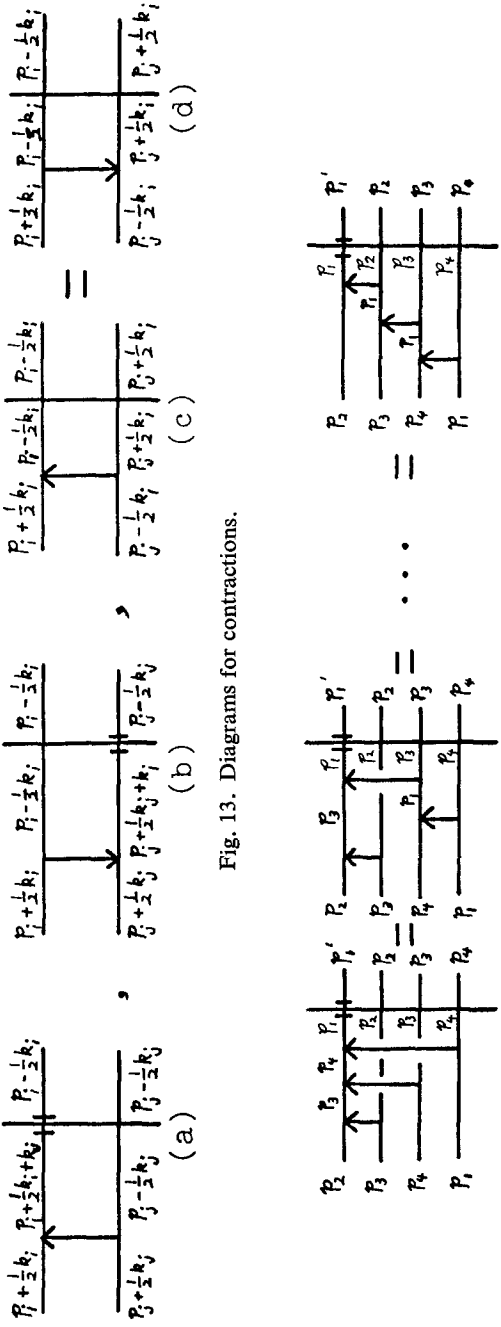

Fig. 13. Diagrams for contractions.

Fig. 14. Diagrams leading to equivalent contractions.

second term in (4.3a) as shown in Fig. 13a, where particle lines other than i and j are not drawn. The arrow indicates the contraction between i and j, and is called the "contracting arrow." The particle lines outside the contracting arrow represent the state of the original component (4.1). The particle lines inside the arrow represent the state obtained by interchanging the roles of the particles. The orientation of the arrow is away from the particle that is diagonalized by the contraction in the density s.state. The arguments on the particle lines are put in as the total momentum is conserved. The argument in the Kronecker symbol is given by the difference between the momenta on the two particle lines on either side of the contracting arrow. In a similar way, the third term in (4.3a) is represented by Fig. 13b, and the second term in (4.3b) by Fig. 13c or 13d.

Here, we note that the contracting arrow is regarded as a kind of interchange operator Q'_{ij} which interchanges the roles of the particles i and j and has an orientation toward i from j, where j is the particle diagonalized by the contraction. For the case including more than two particles, their contraction is performed by iterative application of (4.3), which is represented by a set of contracting arrows arranged in accordance with the order of the successive contractions. However, in the representation of the contraction, there exists an ambiguity in the order of the successive contracting arrows. This originates from the fact that, in order to symmetrize a state, there is an ambiguity in expressing a permutation by the combination of interchange operators. We show this by the example in Fig. 14, where the diagrams correspond to the following combinations of interchange operators: $Q'_{12}Q'_{13}Q'_{14} = Q'_{12}Q'_{34}Q'_{13} = \cdots = Q'_{34}Q'_{23}Q'_{12}$. These represent the same permutation, replacing the order $(\mathbf{p}_1, \mathbf{p}_2, \mathbf{p}_3, \mathbf{p}_4)$ by $(\mathbf{p}_2, \mathbf{p}_3, \mathbf{p}_4, \mathbf{p}_1)$. In order to avoid double counting of the contraction, we must take account of only one of these.

We further remark that, for the contracted part corresponding to (4.2), another diagrammatic representation is possible, as shown in Fig. 15. Here the role of the particles is interchanged on the right side of the Λ line. For the moment, however, our attention is devoted only to the contraction performed on the left side of the Λ line, since after it is investigated, the properties of the right side can be easily obtained through the compensative relation. This type

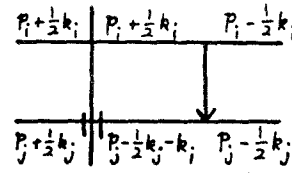

Fig. 15. Another expression for the contraction in Fig. 13a.

of contraction will be used when necessary, and the details of how to take it will be given in Section 5.

4.2. Movement of a Contraction

We now discuss the role of the contraction in the perturbation series (2.33). In (2.33) it seems that all quantum statistical effects have been crowded into the initial Fourier component $\rho_{\mathbf{k}'^s}(\mathbf{p}'^N|\mathbf{p}'^{N-s}; 0)$. However, as was mentioned in Section 2, if an intermediate state is fixed under the condition of a diagonal transition, the quantum statistical effect must appear through this intermediate state. Therefore, in the treatment of the asymptotic time evolution of this system, a method has to be devised for taking account of this effect in our perturbation formalism.

For this purpose, we first note that some of the contractions performed at the initial component also can be regarded as being performed at a time other than $t = 0$. To illustrate this, let us consider the example in Fig. 16, where the contraction is performed in the initial component, $\rho_{\mathbf{k}_1-\mathbf{q},\mathbf{k}_2+\mathbf{q}}(\mathbf{p}_1 + \frac{1}{2}\hbar\mathbf{q}, \mathbf{p}_2 + \frac{1}{2}\hbar\mathbf{q}|\mathbf{p}_3 - \hbar\mathbf{q}, \mathbf{p}^{N-3}; 0)$. The corresponding contribution is

$$
\begin{aligned}
&\rho_{\mathbf{k}_1,\mathbf{k}_2}(\mathbf{p}_1, \mathbf{p}_2|\mathbf{p}_3, \mathbf{p}^{N-3}; t)|_{\lambda^2} \\
&\quad = \left(\frac{-1}{2\pi i}\right)^2 \int_\Gamma dz \int_{\Gamma'} dz'\, e^{-i(z-z')t/\hbar}\lambda^2\Omega^{-1} \\
&\qquad \times \sum_{\mathbf{q}} \frac{1}{E_{\mathbf{p}_1+(1/2)\hbar\mathbf{k}_1,\mathbf{p}_2+(1/2)\hbar\mathbf{k}_2,\mathbf{p}_3} - z} v(q) \\
&\qquad \times \frac{1}{E_{\mathbf{p}_1+\hbar[(1/2)\mathbf{k}_1+\mathbf{k}_2+\mathbf{q}],\mathbf{p}_2-(1/2)\hbar\mathbf{k}_2,\mathbf{p}_3-\hbar\mathbf{q}} - z} \\
&\qquad \times \frac{1}{E_{\mathbf{p}_1-\hbar[(1/2)\mathbf{k}_1-\mathbf{q}],\mathbf{p}_2-(1/2)\hbar\mathbf{k}_2,\mathbf{p}_3-\hbar\mathbf{q}} - z'} v(q) \\
&\qquad \times \frac{1}{E_{\mathbf{p}_1-(1/2)\hbar\mathbf{k}_1,\mathbf{p}_2-(1/2)\hbar\mathbf{k}_2,\mathbf{p}_3} - z'} \\
&\qquad \times \theta\, \delta^{\mathrm{K}}\left(\mathbf{p}_1 + \frac{\hbar}{2}\mathbf{k}_1 - \mathbf{p}_2 + \frac{\hbar}{2}\mathbf{k}_2\right) \\
&\qquad\quad \rho_{\mathbf{k}_1+\mathbf{k}_2}\left(\mathbf{p}_1 + \hbar\left(\mathbf{q} + \frac{1}{2}\mathbf{k}_2\right)\middle|\mathbf{p}_2 - \frac{\hbar}{2}\mathbf{k}_2, \mathbf{p}_3 - \hbar\mathbf{q}; 0\right) \qquad (4.4)
\end{aligned}
$$

In this example, the contraction is performed in the initial component by

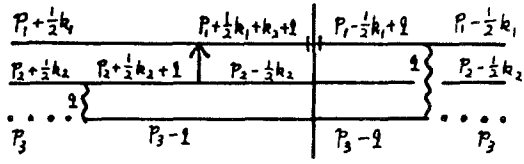

Fig. 16. Diagram corresponding to (4.4).

setting the momenta $\mathbf{p}_1 + (\hbar\mathbf{k}_1/2) = \mathbf{p}_2 - (\hbar\mathbf{k}_2/2)$ irrespective of the potential $v(q)$. Then, if (4.4) is rewritten in the form

$$\begin{aligned}
&\rho_{\mathbf{k}_1,\mathbf{k}_2}(\mathbf{p}_1, \mathbf{p}_2, |\mathbf{p}_3, \mathbf{p}^{N-3}; t)|_{\lambda^2} \\
&= \theta\Omega\, \delta^{\mathrm{K}}\left(\mathbf{p}_1 + \frac{\hbar}{2}\mathbf{q}_1 - \mathbf{p}_2 + \frac{\hbar}{2}\mathbf{k}_2\right)\left(\frac{-1}{2\pi i}\right)^2 \int_\Gamma dz \int_{\Gamma'} dz' \\
&\quad \times e^{-i(z-z')t/\hbar}\lambda^2\Omega^{-2} \sum_{\mathbf{q}} \frac{1}{E_{\mathbf{p}_1+\hbar[(1/2)\mathbf{k}_1+\mathbf{k}_2],\mathbf{p}_2-(1/2)\hbar\mathbf{k}_2,\mathbf{p}_3} - z} v(q) \\
&\quad \times \frac{1}{E_{\mathbf{p}_1+\hbar[(1/2)\mathbf{k}_1+\mathbf{k}_2+\mathbf{q}],\mathbf{p}_2-(1/2)\hbar\mathbf{k}_2,\mathbf{p}_3-\hbar\mathbf{q}} - z} \\
&\quad \times \frac{1}{E_{\mathbf{p}_1-\hbar[(1/2)\mathbf{k}_1-\mathbf{q}],\mathbf{p}_2-(1/2)\hbar\mathbf{k}_2,\mathbf{p}_3-\hbar\mathbf{q}} - z'} v(q) \\
&\quad \times \frac{1}{E_{\mathbf{p}_1-(1/2)\hbar\mathbf{k}_1,\mathbf{p}_2-(1/2)\hbar\mathbf{k}_2,\mathbf{p}_3} - z'} \\
&\quad \times \rho_{\mathbf{k}_1+\mathbf{k}_2}\left(\mathbf{p}_1 + \frac{\hbar}{2}\left(\mathbf{q} + \frac{1}{2}\mathbf{k}_2\right) \middle| \mathbf{p}_2 - \frac{\hbar}{2}\mathbf{k}_2, \mathbf{p}_3 - \hbar\mathbf{q}; 0\right) \qquad (4.5)
\end{aligned}$$

this term can be represented as the diagram in Fig. 17. This shows that the right-hand side of (4.5) is identified with the contracted part $\theta\Omega\, \delta^{\mathrm{K}}(\mathbf{p}_1 + \frac{1}{2}\hbar\mathbf{k}_1 - \mathbf{p}_2 + \frac{1}{2}\hbar\mathbf{k}_2)\rho_{\mathbf{k}_1+\mathbf{k}_2}(\mathbf{p}_1 + \frac{1}{2}\hbar\mathbf{k}_2|\mathbf{p}_2 - \frac{1}{2}\hbar\mathbf{k}_2, \mathbf{p}_3, \mathbf{p}^{N-3}; t)$ of the left-hand

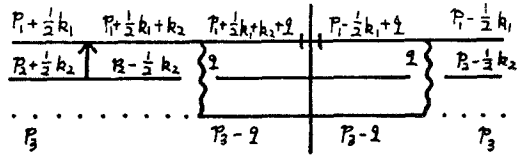

Fig. 17. Diagram corresponding to (4.5). Completely movable contraction.

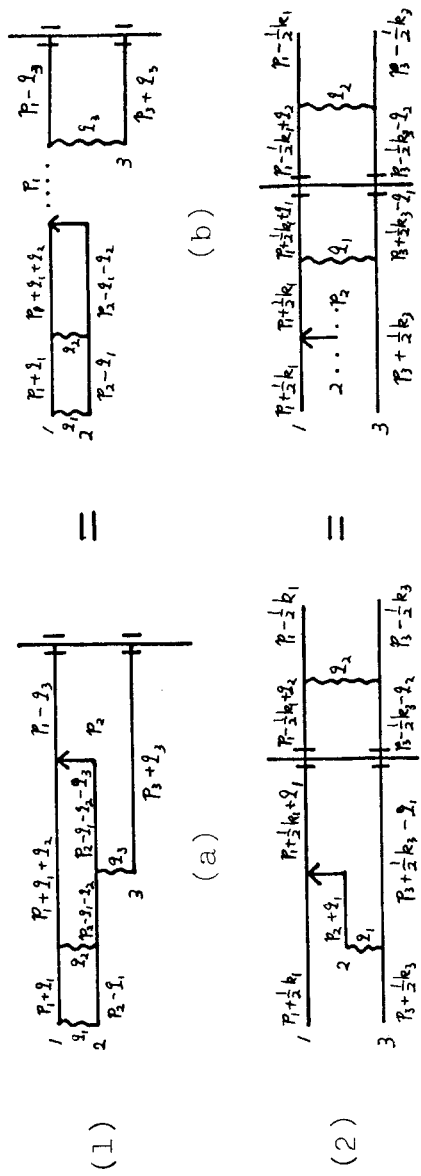

Fig. 18. Examples of the movement of a contraction. (a) Movable contraction; (b) Slideable contraction.

side of (4.6) at time t, and then the contraction can be regarded as having been moved over the potentials. In this movement the role of the particles is interchanged in sliding the contracting arrow from inside to outside the potential, since the contacting arrow plays the role of an interchange operator.

For the examples shown in Fig. 18, the contractions are performed in the destruction part in (1a) and in the propagation-of-correlations part in (2a). In (1a), since the momenta $\mathbf{p}_1 + \hbar\mathbf{q}_1 + \hbar\mathbf{q}_2$ and $\mathbf{p}_2$ relating to the contraction are irrespective of the potential $v(q_3)$, we can rewrite the expression for (1a) in a similar way to (4.5) and get the expression represented by the diagram in (1b). Then, through this contraction, we find that the destruction part in (1a) reduces to two parts, a diagonal fragment and a destruction part. In a similar way, we can also rewrite the diagram (2a) to (2b). However, this contraction cannot be regarded as being performed in the final component $\rho_{\mathbf{k}_1,\mathbf{k}_3}(\mathbf{p}_1, \mathbf{p}_3|\mathbf{p}_2, \mathbf{p}^{N-3}; t)$, because this component has no contractible part between the momenta $\mathbf{p}_1 + (\hbar\mathbf{k}_1/2)$ and $\mathbf{p}_2$. In this case, the propagation-of-correlations part in (2a) does not reduce to any other type of fragment through the contraction.

As shown in these examples, we can classify the movement of a contraction into the following three types: (1) a "completely movable contraction," which is defined as one that can be regarded as being performed in the final component after the complete movement over all potentials, such as in Fig. 17; (2) a "movable contraction," which is defined as one that yields a diagonal s.state through the reduction of the fragment into several types of fragments, such as in Fig. 18(1); and (3) a "slideable contraction," which is defined as one through which the fragment does not reduce to any type of fragment, such as in Fig. 18(2). As will be discussed in the next section, this contraction can move freely over the potential within a fragment. The location of the slideable contraction will be determined so as to be convenient for our applications.

Finally, we refer to the role of the contraction in the asymptotic time dependence of the perturbation series (2.33). For instance, diagram (1a) in Fig. 18 seems to be constructed only from the destruction part, and it has no asymptotic contribution growing with time. However, as is shown in Fig. 18(1b), the reduction yields a diagonal fragment proportional to t. Due to such implicit diagonal transitions due to the quantum statistical effect, the estimation of the time dependence of the perturbation series (2.33) is much more complicated compared with that for the system of distinguishable particles. This complexity, however, can be removed if we reconstruct the perturbation solution (2.33) for $\rho_{\mathbf{k}^r}$ into one for the nonsingular Fourier component $\tilde{\rho}_{\mathbf{k}^r}$, since from the definition of $\tilde{\rho}_{\mathbf{k}^r}$ all reducible parts are removed from it by the contraction. We will discuss such a solution for $\tilde{\rho}_{\mathbf{k}^r}$ in the following section.

5. SOLUTION FOR $\tilde{\rho}_{\mathbf{k}^r}(t)$ AND ITS APPLICATIONS

5.1. Solution for $\tilde{\rho}_{\mathbf{k}^r}(t)$

We give a systematic method for reconstructing the solution for $\tilde{\rho}_{\mathbf{k}^r}(t)$ from the perturbation series (2.33).

This reconstruction can be achieved by the use of our diagrammatic method as follows: First, we perform the contractions at the initial Fourier component in the perturbation series (2.33), and let all movable and completely movable contractions move over the potentials as far to the outside as possible. By comparing this result with the terms on the left-hand side of (2.33) in which the contractions are performed at time t, we find a set of solutions for $\tilde{\rho}_{\mathbf{k}^r}(t)$ in which all diagonal fragments are explicitly separated.

We notice that in these solutions all slideable contractions can be moved freely within each fragment, since they give no reduction of the fragments and thus they merely play the role of interchanging operators. It is convenient to classify these slideable contractions into two groups: "external degenerating contractions" (called external contractions), which connect with the completely vacuum line, such as in Fig. 18(2b); and "internal degenerating contractions" (called internal contractions), which never connect with the completely vacuum line wherever the arrow is located within the fragment, such as in Fig. 19.

An external contraction indicates a degenerating effect between a particle in the collision and a particle in the background of this collision, which behaves as the Fermi sea of the Pauli exclusion principle for fermion case. This contraction can be easily included in our diagrams by merely putting arrows on the unsymmetrized diagram given in the previous section.

An internal contraction indicates a degenerating effect between the particles in a collision, such as an exchange collision. This contraction can be further classified into two groups, a contraction for a bubble and a contraction for a skeleton. The former is defined as one that is associated with a bubble, such as in Fig. 19, and the latter as one that never yields a bubble by its movement within the fragment.

With the aid of these classifications and of the compensative relation, we can build up the quantum statistical collision s.operator on the same basis

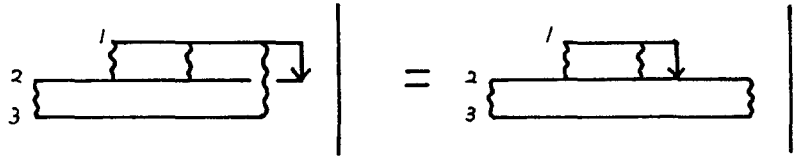

Fig. 19. Example of an internal contraction.

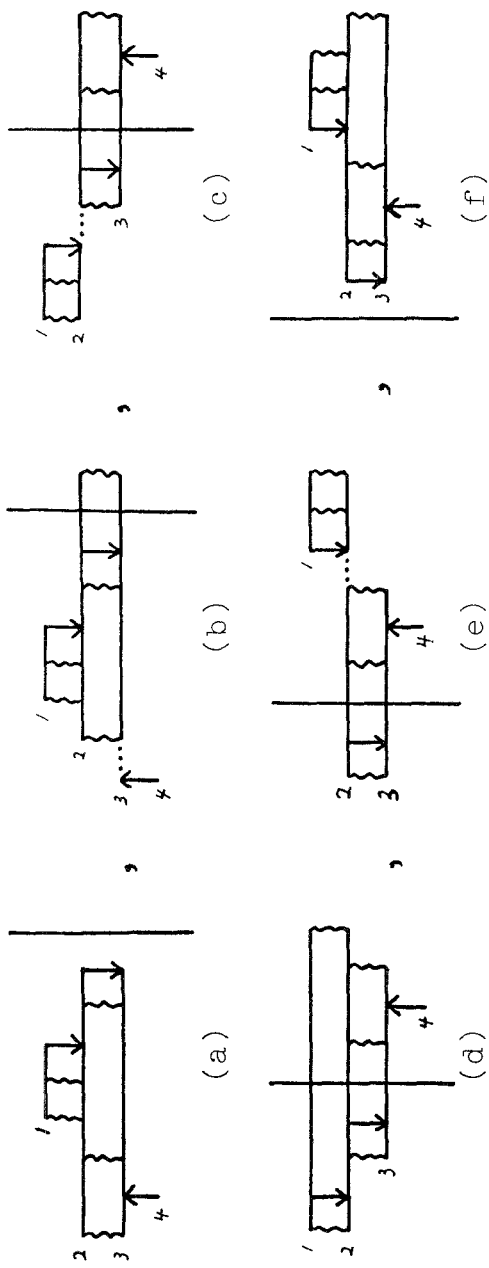

Fig. 20. Compensative diagrams with contracting arrows.

Fig. 21. Diagrams with the same contribution.

as in the unsymmetrized case, i.e., using the skeleton fragment, the bubble, and the inactivated diagonal fragment. For example, starting with diagram (a) in Fig. 20, we can obtain all compensative diagrams in Fig. 20 by the rule of compensation. To get diagram (e) from (d) we use the fact that the diagrams in Fig. 21 give the same contribution. Furthermore, the diagrams in Fig. 20 can be decomposed into the o.p. representation. For example, the diagrams proportional to l^{-2} are shown in Fig. 22, where we have slid the contractions for a bubble and for a skeleton to the outside on the right diagonal fragment so as to get the same topological structure as the left diagonal fragment.

5.2. Extension for a Linearized Hydrodynamic System

We now extend our formalism to an inhomogeneous system in which the characteristic lengths of the system satisfy the inequalities

$$L_h \gg L_r \gg a, \qquad L_h \gg \lambda_B \tag{5.1}$$

where L_h is the hydrodynamic length, L_r is the mean free path, a is the molecular length, and λ_B is the de Broglie wavelength. We further restrict the system so that the deviation of the local density from the average density c is very small [see (5.7)]. This assumption implies that it is sufficient for us to make a theory linear in this deviation.

For such a linearized hydrodynamic system, we need to extend the concept of the vacuum component, such that it consists of the Fourier component $\rho_k(\mathbf{p}|\mathbf{p}^{N-1})$ having a single nonzero wave vector. This new vacuum state is indicated by a single excited line in our diagrammatic method, where all the previous concepts of creation part, diagonal fragment, destruction part, and so on remain, changing only the meaning of the vacuum component. Some typical diagonal fragments for this system are shown in Fig. 25.

5.3. Derivation of the Asymptotic Kinetic Equation

Following our diagrammatic method, we consider two simple examples.

Homogeneous system: Let us first derive the kinetic equation for the single-particle momentum distribution function in a weakly coupled system in the limit

$$\lambda \to 0, \qquad t \to \infty, \qquad \lambda^2 t = \text{const.} \tag{5.2}$$

For this case, the o.s. diagonal skeleton fragment is given as shown in Fig. 23, and thus the summation of all possible diagrams contributing to the N-particle momentum distribution function $\phi_N(\mathbf{p}^N, t) = \rho_0(|\mathbf{p}^N; t) = \tilde{\rho}_0(|\mathbf{p}^N; t)$

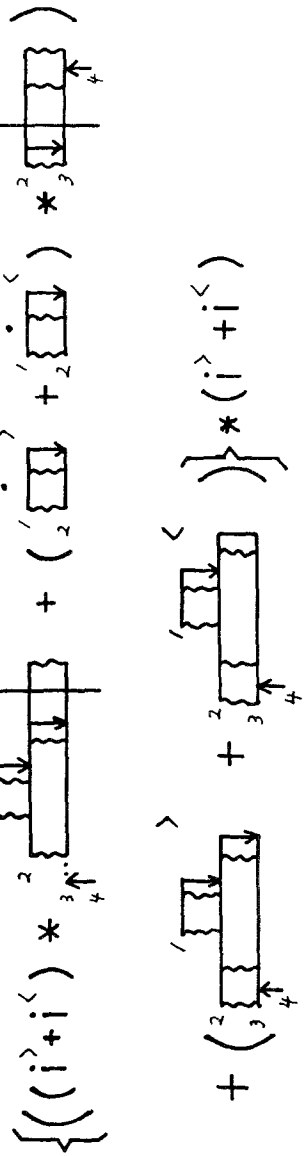

Fig. 22. Compensative diagrams obtained from Fig. 20 as those proportional to I^{-2}.

Fig. 23. One-sided diagonal skeleton diagram contributing in the weakly coupled homogeneous system.

is given in the o.p. representation shown in Fig. 24. The corresponding expression for the diagram in Fig. 24 is

$$\phi_N(\mathbf{p}^N, t) = \left(\frac{1}{2\pi i}\right)^2 \int_{-\infty}^{+\infty} dE \int_\gamma dl\, e^{-ilt/\hbar} \sum_{n=0}^{\infty} \Delta^{(0)}_{\mathbf{p}^N,E}(l) \frac{1}{l} \left[\tilde{\chi}^{(2)}_{\mathbf{p}^N,E}(l) \frac{1}{l}\right]^n \times \prod_{k=0}^{N} \phi_1(\mathbf{p}_k, 0) \tag{5.3}$$

where

$$\begin{aligned}\tilde{\chi}^{(2)}_{\mathbf{p}^N,E}(l) = \lambda^2\Omega^{-2} \sum_{i<j}^{N} \sum_{\mathbf{q}} \left[v(q) + \theta v\left(\left|\frac{\mathbf{p}_i}{\hbar} - \frac{\mathbf{p}_j}{\hbar} + \mathbf{q}\right|\right)\right] v(q) \Delta^{(0)}_{\mathbf{p}_i+\hbar\mathbf{q},\mathbf{p}_j-\hbar\mathbf{q},\mathbf{p}^{N-2},E}(l) \\ \times \left\{\left[1 + \theta \sum_{r=1}^{N} \delta^{\mathrm{K}}(\mathbf{p}_i - \mathbf{p}_r)\right]\left[1 + \theta \sum_{s=1}^{N} \delta^{\mathrm{K}}(\mathbf{p}_j - \mathbf{p}_s)\right]\right. \\ \times \exp[\hbar\mathbf{q}(\partial/\partial\mathbf{p}_i - \partial/\partial\mathbf{p}_j)] \\ \left. - \left[1 + \theta \sum_{r=1}^{N} \delta^{\mathrm{K}}(\mathbf{p}_i + \hbar\mathbf{q} - \mathbf{p}_r)\right]\left[1 + \theta \sum_{s=1}^{N} \delta^{\mathrm{K}}(\mathbf{p}_j - \hbar\mathbf{q} - \mathbf{p}_s)\right]\right\}\end{aligned} \tag{5.4}$$

$$\Delta^{(0)}_{\mathbf{p}^N,E}(l) = \frac{1}{E_{\mathbf{p}^N} - E - \frac{1}{2}l} - \frac{1}{E_{\mathbf{p}^N} - E + \frac{1}{2}l} \tag{5.5}$$

and the displacement operator $\exp(\hbar\mathbf{q}\,\partial/\partial\mathbf{p})\, F(\mathbf{p}) = F(\mathbf{p} + \hbar\mathbf{q})$ is used. Then, evaluating the contribution around the poles $l = 0$ in (5.3), integrating over the momenta except for $\mathbf{p}_1$ of the fixed particle, and taking the time derivative, we get the well-known equation for the limit (5.2) as

$$\begin{aligned}\partial_t \phi_1(\mathbf{p}_1, t) = \frac{(2\pi)^3 c\lambda^2}{\hbar} \int d\mathbf{p}_2 \int d\mathbf{q}\, v(q) \left[v(q) + \theta v\left(\left|\frac{\mathbf{p}_1}{\hbar} - \frac{\mathbf{p}_2}{\hbar} + \mathbf{q}\right|\right)\right] \\ \times 2\pi\, \delta(E_{\mathbf{p}_1+\hbar\mathbf{q}} + E_{\mathbf{p}_2-\hbar\mathbf{q}} - E_{\mathbf{p}_1} - E_{\mathbf{p}_2}) \\ \times \{\phi_1(\mathbf{p}_1 + \hbar\mathbf{q}, t)\phi_1(\mathbf{p}_2 - \hbar\mathbf{q}, t)[1 + \theta h^3 c\phi_1(\mathbf{p}_1, t)] \\ \times [1 + \theta h^3 c\phi_1(\mathbf{p}_2, t)] \\ - \phi_1(\mathbf{p}_1, t)\phi_1(\mathbf{p}_2, t)[1 + \theta h^3 c\phi_1(\mathbf{p}_1 + \hbar\mathbf{q}, t)] \\ \times [1 + \theta h^3 c\phi_1(\mathbf{p}_2 - \hbar\mathbf{q}, t)]\}\end{aligned} \tag{5.6}$$

Linearized hydrodynamic system: As a second example, we consider a weakly coupled inhomogeneous system under the condition (5.2). Our interest is now in the derivation of the linearized Boltzmann equation for the reduced function $\rho^{(1)}_{\mathbf{k}}(\mathbf{p}_1, t)$, which is the Fourier component of the deviation of the local density from the average density c, i.e.,

$$\rho^{(1)}_{\mathbf{k}}(\mathbf{p}_1, t) = \frac{1}{(2\pi)^3 c} \int d\mathbf{x}_1\, [\exp(-i\mathbf{k}\mathbf{x}_1)][f_1(\mathbf{x}_1, \mathbf{p}_1, t) - c\phi_1(\mathbf{p}_1, t)] \tag{5.7}$$

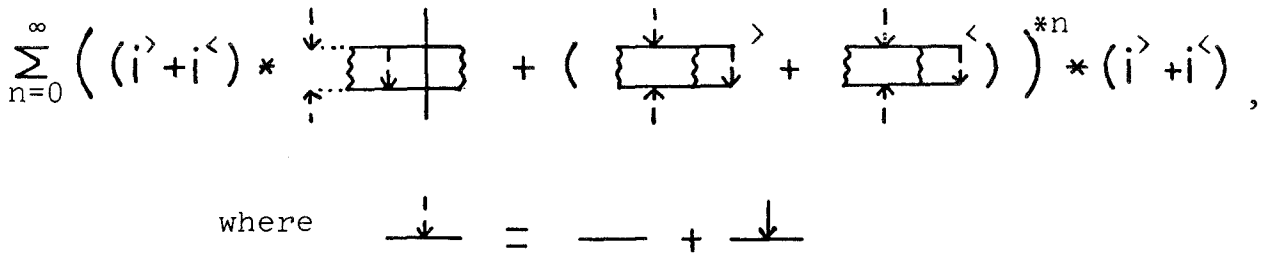

Fig. 24. Summation of all diagrams contributing in the weakly coupled homogeneous system.

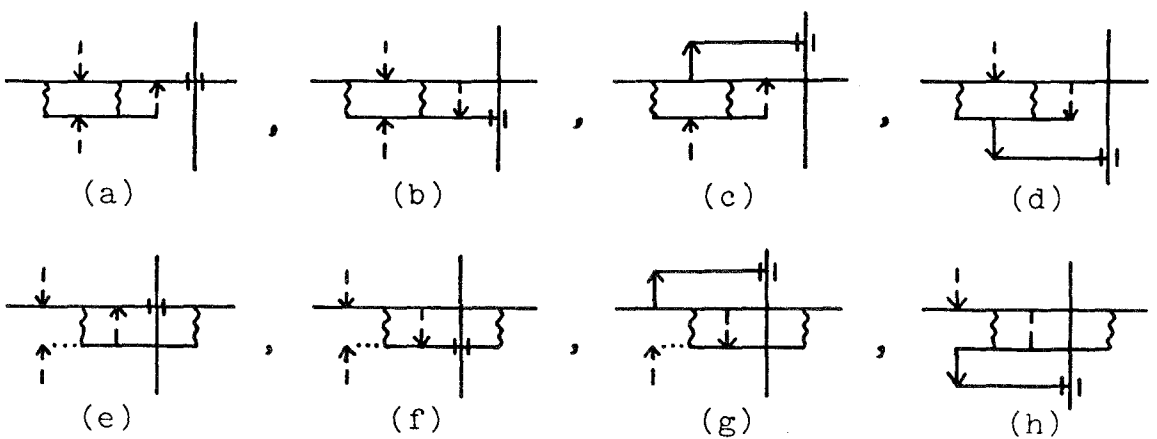

Fig. 25. Diagonal fragments contributing in the weakly coupled inhomogeneous system.

To derive this equation under the condition (5.1), we first notice that the typical wave vector k ($\sim 1/L_h$) is much smaller than the momentum transfer of the potential $\hbar q$ ($\sim \hbar/a$) and the momentum p ($\sim \hbar/\lambda_B$). For this system, the diagonal fragments, which reduce to the diagrams in Fig. 24 by setting $\mathbf{k} = 0$, may give the main contribution to $\rho_{\mathbf{k}}(\mathbf{p}_1|\mathbf{p}^{N-1}; t)$. Such diagonal fragments can be obtained by replacing one of the vacuum lines in Fig. 24 by an excited line. The results are shown in Fig. 25, where the left fragment and the t.s. diagonal fragment are drawn. The corresponding expression for diagram (a) in Fig. 25 is

$$
\begin{aligned}
I_a = \left(\frac{1}{2\pi i}\right)^2 \int_{-\infty}^{+\infty} dE \int_{\gamma} dl\, e^{-ilt/\hbar} \Bigg\{ & \frac{1}{l - (\hbar/m)\mathbf{k}\mathbf{p}_1} \left[-G^{(s)}_{\mathbf{p}_1,\mathbf{k},E}(l)\right] \frac{1}{l - (\hbar/m)\mathbf{k}\mathbf{p}_1} \\
& \times \left[\frac{1}{E_{\mathbf{p}_1+(1/2)\hbar\mathbf{k},\mathbf{p}^{N-1}} - E - \frac{1}{2}l} - \frac{1}{E_{\mathbf{p}_1+(1/2)\hbar\mathbf{k},\mathbf{p}^{N-1}} - E + \frac{1}{2}l} \right] \\
& + \frac{1}{l - (\hbar/m)\mathbf{k}\mathbf{p}_1} \frac{1}{E_{\mathbf{p}_1+(1/2)\hbar\mathbf{k},\mathbf{p}^{N-1}} - E - \frac{1}{2}l} G^{(s)}_{\mathbf{p}_1,\mathbf{k},E}(l) \\
& \times \frac{1}{E_{\mathbf{p}_1+(1/2)\hbar\mathbf{k},\mathbf{p}^{N-1}} - E - \frac{1}{2}l} \Bigg\} \rho_{\mathbf{k}}(\mathbf{p}_1|\mathbf{p}^{N-2}; 0)
\end{aligned}
\tag{5.8}
$$

where

$$
\begin{aligned}
G^{(s)}_{\mathbf{p}_1,\mathbf{k},E}(l) = \lambda^2 \Omega^{-2} \sum_i \sum_{\mathbf{q}} v(q) & \frac{1}{E_{\mathbf{p}_1+(1/2)\hbar\mathbf{k}+\hbar\mathbf{q},\mathbf{p}_i-\hbar\mathbf{q},\mathbf{p}^{N-2}} - E - \frac{1}{2}l} \\
& \times \left[1 + \theta \sum_{r=1}^{N} \delta^{\mathrm{K}}\left(\mathbf{p}_1 + \frac{\hbar}{2}\mathbf{k} + \hbar\mathbf{q} - \mathbf{p}_r\right)\right] \\
& \times \left[1 + \theta \sum_{s=1}^{N} \delta^{\mathrm{K}}(\mathbf{p}_i - \hbar\mathbf{q} - \mathbf{p}_s)\right] \\
& \times \left[v(q) + \theta v\left(\left|\frac{\mathbf{p}_1}{\hbar} - \frac{\mathbf{p}_i}{\hbar} + \frac{1}{2}\mathbf{k} + \mathbf{q}\right|\right)\right]
\end{aligned}
\tag{5.9}
$$

Under the assumptions of (5.1), we may approximate $\mathbf{p}_1 \pm (\hbar\mathbf{k}/2) \sim \mathbf{p}_1$ in (5.8) and may expand $[l - (\hbar\mathbf{k}\mathbf{p}_1/m)]^{-1}$ as

$$
\frac{1}{l - (\hbar/m)\mathbf{k}\mathbf{p}_1} = \frac{1}{l} \sum_{j=1}^{\infty} \left(\frac{\hbar\mathbf{k}\mathbf{p}_1}{m} \frac{1}{l}\right)^j \tag{5.10}
$$

Then, evaluating the contributions from the poles at $l = 0$ under the condition (5.2), we get

$$
\begin{aligned}
I_a \simeq \sum_{j=1}^{\infty} \frac{1}{j!} \sum_{n=0}^{j-1} & \left(-it\frac{\mathbf{k}\mathbf{p}_1}{m}\right)^{j-n-1} \left(\frac{-i\lambda^2 t}{\hbar}\right) \left[-G^{(s)}_{\mathbf{p}_1,0,E_{\mathbf{p}^N}}(+i0)\right] \\
& \times \left(-it\frac{\mathbf{k}\mathbf{p}_1}{m}\right)^n \rho_{\mathbf{k}}(\mathbf{p}_1|\mathbf{p}^{N-1}; 0)
\end{aligned}
\tag{5.11}
$$

Similar terms are obtained for the diagrams in Figs. 25b–25h and also for the right diagonal fragments. Furthermore, diagrams consisting of more than one diagonal fragment are evaluated in a similar way. Then we get the solution for $\rho_{\mathbf{k}}(\mathbf{p}_1|\mathbf{p}^{N-1}; t)$. Then integrating over the momenta except for $\mathbf{p}_1$ of the fixed particle and taking the time derivative, we obtain the linearized Boltzmann equation for $\rho_{\mathbf{k}}^{(1)}(\mathbf{p}_1, t)$:

$$
\begin{aligned}
&\partial_t \rho_{\mathbf{k}}^{(1)}(\mathbf{p}_1) + i\frac{\mathbf{k}\mathbf{p}_1}{m}\rho_{\mathbf{k}}^{(1)}(\mathbf{p}_1) \\
&= \frac{(2\pi)^3 c\lambda^2}{\hbar}\int d\mathbf{p}_2 \int d\mathbf{q}\left[v(q) + \theta v\left(\left|\frac{\mathbf{p}_1}{\hbar} - \frac{\mathbf{p}_2}{\hbar} + \mathbf{q}\right|\right)\right] \\
&\quad \times 2\pi\,\delta(E_{\mathbf{p}_1+\hbar\mathbf{q}} + E_{\mathbf{p}_2-\hbar\mathbf{q}} - E_{\mathbf{p}_1} - E_{\mathbf{p}_2}) \\
&\quad \times (\{\phi_1(\mathbf{p}_2 - \hbar\mathbf{q})[1 + \theta h^3 c\phi_1(\mathbf{p}_2)][1 + \theta h^3 c\phi_1(\mathbf{p}_1)] \\
&\quad - \theta h^3 c[1 + \theta h^3 c\phi_1(\mathbf{p}_2 - \hbar\mathbf{q})]\phi_1(\mathbf{p}_2)\phi_1(\mathbf{p}_1)\}\rho_{\mathbf{k}}^{(1)}(\mathbf{p}_1 + \hbar\mathbf{q}) \\
&\quad - \{\phi_1(\mathbf{p}_2)[1 + \theta h^3 c\phi_1(\mathbf{p}_2 - \hbar\mathbf{q})][1 + \theta h^3 c\phi_1(\mathbf{p}_1 + \hbar\mathbf{q})] \\
&\quad - \theta h^3 c[1 + \theta h^3 c\phi_1(\mathbf{p}_2)]\phi_1(\mathbf{p}_2 - \hbar\mathbf{q})\phi_1(\mathbf{p}_1 + \hbar\mathbf{q})\}\rho_{\mathbf{k}}^{(1)}(\mathbf{p}_1) \\
&\quad + \{\phi_1(\mathbf{p}_1 + \hbar\mathbf{q})[1 + \theta h^3 c\phi_1(\mathbf{p}_1)][1 + \theta h^3 c\phi_1(\mathbf{p}_2)] \\
&\quad - \theta h^3 c[1 + \theta h^3 c\phi_1(\mathbf{p}_1 + \hbar\mathbf{q})]\phi_1(\mathbf{p}_1)\phi_1(\mathbf{p}_2)\}\rho_{\mathbf{k}}^{(1)}(\mathbf{p}_2 - \hbar\mathbf{q}) \\
&\quad - \{\phi_1(\mathbf{p}_1)[1 + \theta h^3 c\phi_1(\mathbf{p} + \hbar\mathbf{q})][1 + \theta h^3 c\phi_1(\mathbf{p}_2 - \hbar\mathbf{q})] \\
&\quad - \theta h^3 c[1 + \theta h^3 c\phi_1(\mathbf{p}_1)]\phi_1(\mathbf{p}_1 + \hbar\mathbf{q})\phi_1(\mathbf{p}_2 - \hbar\mathbf{q})\}\rho_{\mathbf{k}}^{(1)}(\mathbf{p}_2)) \quad (5.12)
\end{aligned}
$$

where all functions $\rho_{\mathbf{k}}^{(1)}$ and ϕ_1 are at time t. By putting $\theta = -1$ for the fermion case, this equation coincides with the equation derived by Résibois and Dagonnier.[16]

6. CONCLUSION

We have formulated the perturbation theory of the two-resolvent method in a superspace and given a diagrammatic method so that a description parallel to the one-resolvent method is possible with the use of the concepts of the creation part, the diagonal part with collision s.operators, the destruction part, and the propagation-of-correlations part. Our method offers practical applications to physical systems and improves the usefulness of the two-resolvent method for large quantum systems. We have further developed our diagrammatic method so as to be able to treat the quantum statistical effect through the concept of a moving contraction. For a quantum statistical system, it has been shown how the contracting procedure given here is much simpler than that of our previous work[14] with the one-resolvent method, and this simplicity enables us to treat the complicated quantum statistical effect more easily.

Finally, we comment on the relation of the extension of our theory to a more general hydrodynamic system without the linearizing condition, to the recent developments of the one-resolvent method. For such a system, Severne[6] developed the one-resolvent method based on the cluster decomposition of the correlation function, and an extension of this theory to the quantum statistical system has been attempted by Balescu[10] based on the correlation pattern. In order to develop our theory in this direction, we have to extend the concept of the vacuum component, which is now defined by the Fourier component $\rho_{\mathbf{k}}{}^{r}$ having wave vectors smaller than the inverse of the hydrodynamic length $L_{\hbar}$. This definition implies that the vacuum component for the hydrodynamic system can be factorized as

$$\rho_{\mathbf{k}}{}^{r}(\mathbf{p}^{r}|\mathbf{p}^{N-r}) = \prod_{i=1}^{r}\prod_{j=r+1}^{N}\rho_{\mathbf{k}_i}^{(1)}(\mathbf{p}_i)\phi_1(\mathbf{p}_j) \tag{6.1}$$

with $|\mathbf{k}_i| \lesssim L_{\hbar}^{-1}$ for $i = 1,\ldots, r$. For such a case, the quasidiagonal s.state, which is defined as an off-diagonal s.state with small gaps of momenta of the order of $\hbar L_{\hbar}^{-1}$, plays a central role similar to the diagonal s.state in the homogeneous system. Consequently, the quantum statistical effect also appears through this quasidiagonal s.state. Then, an extension of the contraction is required so as to take account of the effect of the reduction of the Fourier component having large wave vectors into one having small wave vectors by interchanging the role of particles in the density s.state. This is achieved by collecting the terms

$$\sum_{|\mathbf{k}_j-\mathbf{k}'|\le L_{\hbar}^{-1}}{}' \theta\,\delta^{\mathrm{K}}\left(\hbar\mathbf{k}_j - \hbar\mathbf{k}' + \mathbf{p}_i + \frac{\hbar}{2}\mathbf{k}_i - \mathbf{p}_j + \frac{\hbar}{2}\mathbf{k}_j\right) \times \rho_{\mathbf{k}_i+\mathbf{k}',\mathbf{k}_j-\mathbf{k}'}\left(\mathbf{p}_i + \frac{\hbar}{2}\mathbf{k}', \mathbf{p}_j - \frac{\hbar}{2}\mathbf{k}', \mathbf{p}^{r-2}|\mathbf{p}^{N-r}\right) \tag{6.2}$$

from the first term $\rho'_{\mathbf{k}}{}^{r}$ of the contraction formulas (4.3).[5] In (6.2), the prime on the summation sign indicates the exclusion of $\mathbf{k}' = 0$. We call this new reduction "quasicontraction." In our diagrammatic method, the quasicontraction (6.2) is represented as shown in Fig. 26, where particle lines other than i and j are not drawn. A typical one-sided "quasidiagonal fragment" is shown in Fig. 27.

[5] We can show that the summation of the contracted parts in (4.3) with (6.2) is the same as the term obtained from Balescu's symmetrization operator $P_2(i;j)$ acting on $\pi_2(i;j)$ in Ref. 10.

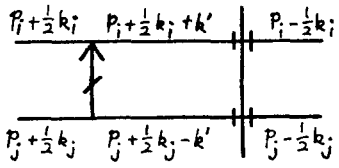

Fig. 26. Diagram corresponding to (6.2).

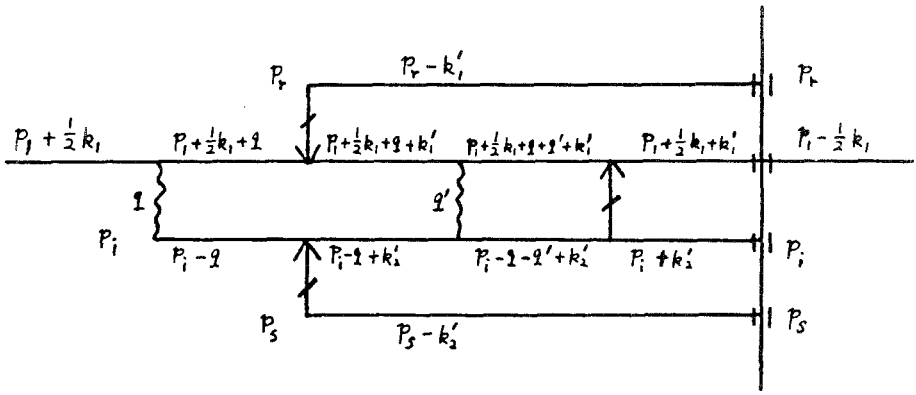

Fig. 27. Typical one-sided quasidiagonal fragment in the hydrodynamic system.

Under such an extension, we may expand our two-resolvent method into a formalism including nonlinear hydrodynamic systems. The details of this formalism will be given subsequently in this series.

APPENDIX A

In the appendix, we give the reduction formulas for exposing all the poles at $l = 0$ in a diagonal s.state. We first introduce a "diagonal s.state function" (d.s. function) $\Psi^{\cdot}$ by

$$\Psi^{\cdot}(\alpha_0, \alpha_1, \ldots, \alpha_m; \alpha_0', \alpha_1', \ldots, \alpha_n' | z, z')$$
$$= \frac{1}{\alpha_0 - z} G_1(z) \frac{1}{\alpha_1 - z} G_2(z) \cdots \frac{1}{\alpha_{m-1} - z} G_m(z) \frac{1}{\alpha_m - z}$$
$$\times \frac{1}{\alpha_{n'} - z'} G_{n'}(z') \frac{1}{\alpha_{n-1}' - z'} \cdots G_{2'}(z') \frac{1}{\alpha_1' - z'} G_{1'}(z') \frac{1}{\alpha_0' - z'} \quad \text{(A1)}$$

where $\alpha_i = \alpha_j' = \alpha$ for all i and j, and the abbreviations α_i for E_{α_i} and G_i for G_{α_i} are used. The tetradic element $(\alpha; \alpha | D^{>}(z) D^{<}(z') | \alpha; \alpha)$ in (3.2) can be expressed by the summation of the d.s. functions over all m and n. The d.s. function obeys the following reduction formulas:

$$\Psi^{\cdot}(\alpha_0, \ldots, \alpha_m; \alpha_0', \ldots, \alpha_n' | z, z')$$
$$= \frac{1}{z - z' - \alpha_{00}} [G_{1'} \Psi^{\cdot}(\alpha_0, \ldots, \alpha_m; \alpha_1', \ldots, \alpha_n' | z, z')$$
$$+ (-G_1) \Psi^{\cdot}(\alpha_1, \ldots, \alpha_n; \alpha_0', \ldots, \alpha_n' | z, z')] \quad \text{(A2)}$$
$$\Psi^{\cdot}(\alpha_0, \ldots, \alpha_m; \alpha_0', \ldots, \alpha_n' | z, z')$$
$$= [\Psi^{\cdot}(\alpha_0, \ldots, \alpha_m; \alpha_0', \ldots, \alpha_{n-1}' | z, z') G_{n'}$$
$$+ \Psi^{\cdot}(\alpha_0, \ldots, \alpha_{m-1}; \alpha_0', \ldots, \alpha_n' | z, z')(-G_m)] \frac{1}{z - z' - \alpha_{mn}} \quad \text{(A3)}$$

where $\alpha_{ij} \equiv \alpha_i - \alpha_j'$. By iterating (A2), we get

$$\begin{aligned}\Psi(\alpha_0,\ldots,\alpha_m;\alpha_0',\ldots,\alpha_n'|z,z') &= \frac{1}{z-z'-\alpha_{00}} G_1' \frac{1}{z-z'-\alpha_{01}} [G_0\Psi(\alpha_0,\ldots,\alpha_m;\alpha_2',\ldots,\alpha_n'|z,z') \\ &+ (-G_1)\Psi(\alpha_1,\ldots,\alpha_m;\alpha_1',\ldots,\alpha_n'|z,z')] \\ &+ \frac{1}{z-z'-\alpha_{00}}(-G_1)\frac{1}{z-z'-\alpha_{10}}[G_1'\Psi(\alpha_1,\ldots,\alpha_m;\alpha_1',\ldots,\alpha_m'|z,z') \\ &+ (-G_2)\Psi(\alpha_2,\ldots,\alpha_m;\alpha_0',\ldots,\alpha_n'|z,z')] \qquad \text{(A4)}\end{aligned}$$

By iterating this formula until all possible factors $(z - z' - \alpha_{ij})^{-1}$ are exposed, we get the decomposition of the d.s. function as the summation of $(m + n)!/(m!\, n!)$ terms, each of them having the factor

$$\frac{1}{\alpha_r - z} G_{r+1} \frac{1}{\alpha_{r+1} - z} G_{r+2} \cdots \frac{1}{\alpha_{m-1} - z} G_m \frac{1}{\alpha_m - z} \qquad (0 \leqslant r \leqslant m) \quad \text{(A5a)}$$

or

$$-\frac{1}{\alpha_s - z'} G_{s'+1} \frac{1}{\alpha_{s+1}' - z'} G_{s'+2} \cdots \frac{1}{\alpha_{n-1}' - z'} G_{n'} \frac{1}{\alpha_n' - z'} \qquad (0 \leqslant s \leqslant n)$$

(A5b)

on the right side and having the remaining diagonal fragments $-G_i$ and G_j with the factor $(z - z' - \alpha_{ij})^{-1}$. In the product of these remaining factors, there appear all terms corresponding to those permutations among the diagonal fragments $-G_i$ and G_j' that are on opposite sides of the Λ line (no permutations among the fragments on the same side of the Λ line appear, since there already is order among them). Then, if each fragment of a diagram is arranged in accordance with the order of this decomposition, the ordered product representation is obtained.

Furthermore, if (A3) is used instead of (A2), a similar decomposition is obtained, but in this case, one of the two factors similar to (A5) is located on the left side in each term. Then this new decomposition leads to another ordered product representation such as in Fig. 7.

APPENDIX B. Derivation of (3.29)

By evaluating the poles at $l = 0$ in (3.24), we have

$$\rho_{0,E}(|\mathbf{p}^N;t) = \frac{1}{2\pi i} \sum_{\mathbf{p}'^N} \sum_{m=0}^{\infty} \frac{1}{m!} \left(\frac{-it}{\hbar} + \partial_l\right)^m \chi_E{}^m(l)\Delta_E(l)\rho_0(|\mathbf{p}'^N;0)|_{l=+i0} \qquad \text{(B1)}$$

where $\partial_l \equiv \partial/\partial l$ and the bra and ket notations have been abbreviated and the

destruction part has been omitted for simplicity (this part leads to no new aspect in the resultant equation). Differentiating (B1) with respect to t, we get

$$\begin{aligned} & i\hbar\, \partial_t \rho_{0,E}(|\mathbf{p}^N; t) \\ & \quad = \frac{1}{2\pi i} \sum_{\mathbf{p}'^N} \sum_{m=0}^{\infty} \sum_{r=0}^{m} \sum_{s=0}^{m-r} \frac{1}{r!\, s!\, (m-r-s)!} \left(\frac{-it}{\hbar}\right)^r \\ & \quad \times [\partial_l{}^s \chi_E(l)][\partial_l^{m-r-s} \chi_E{}^m(l) \Delta_E(l)] \rho_0(|\mathbf{p}'^N; 0)|_{l=+i0} \end{aligned} \tag{B2}$$

On the other hand, from (3.28) we have

$$\chi_E(l) = \frac{2\pi}{\hbar} \int_0^{\infty} d\tau\, {}^{+il\tau/\hbar} \chi_E{}'(\tau) \tag{B3}$$

and thus

$$[\partial_l{}^s \chi_E(l)]_{l=+i0} = \frac{2\pi}{\hbar} \int_0^{\infty} d\tau \left(\frac{i\tau}{\hbar}\right)^s \chi_E{}'(\tau) \tag{B4}$$

Substituting (B4) into (B2), we have

$$\begin{aligned} & i\hbar\, \partial_t \rho_{0,E}(|\mathbf{p}^N; t) \\ & \quad = \frac{2\pi}{\hbar} \int_0^{\infty} d\tau \sum_{\mathbf{p}'^N} \chi_E{}'(\tau) \frac{1}{2\pi i} \sum_{m=0}^{\infty} \sum_{r=0}^{m} \sum_{s=0}^{m-r} \frac{1}{r!\, s!\, (m-r-s)!} \\ & \quad \times \left(\frac{-it}{\hbar}\right)^r \left(\frac{i\tau}{\hbar}\right)^s [\partial_l^{m-r-s} \chi_E{}^m(l) \Delta_E(l)] \rho_0(|\mathbf{p}'^N; 0)|_{l=+i0} \\ & \quad = \frac{2\pi}{\hbar} \int_0^{\infty} d\tau \sum_{\mathbf{p}'^N} \chi_E{}'(\tau) \frac{1}{2\pi i} \sum_{m=0}^{\infty} \frac{1}{m!} \left[\frac{-i}{\hbar}(t-\tau) + \partial_l\right]^m \\ & \quad \times \chi_E{}^m(l) \Delta_E(l) \rho_0(|\mathbf{p}'^N; 0)|_{l=+i0} \end{aligned} \tag{B5}$$

Then, substituting (B1) into the right-hand side of (B5), we arrive at the asymptotic master equation,

$$i\hbar\, \partial_t \rho_{0,E}(|\mathbf{p}^N; t) = \frac{2\pi}{\hbar} \int_0^{\infty} d\tau \sum_{\mathbf{p}'^N} \chi_E{}'(\tau) \rho_{0,E}(|\mathbf{p}'^N; t-\tau) \tag{B6}$$

APPENDIX C

We show here that if the reduced properties of the system are of interest, it is enough to treat only the connected diagram containing the fixed particle.

To illustrate this, we consider the example of the single momentum distribution function defined in (2.23), i.e.,

$$\phi_1(\mathbf{p}_1, t) = (\hbar^3\Omega^{-1})^{N-1} \sum_{\mathbf{p}'^{N-1}} \sum_{\mathbf{p}'^N} \left(\frac{-1}{2\pi i}\right)^2 \int_\Gamma dz \int_{\Gamma'} dz'\, e^{-i(z-z')t/\hbar}$$

$$\times (\mathbf{p}^N; \mathbf{p}^N | \mathscr{P} R^>(z) R^<(z') \mathscr{P} | \mathbf{p}'^N; \mathbf{p}'^N) \prod_{i=1}^{N} \phi_1(\mathbf{p}_i', 0) \qquad \text{(C1)}$$

where it is assumed for simplicity that only the vacuum component ρ_0 does not vanish at the initial time $t = 0$. The summation $\sum_{\mathbf{p}^{N-1}}$ in (C1) is taken over the momenta of the particles, except for the fixed particle 1. Each diagram contributing to (C1) consists in general of several subgroups connected partially through their interactions. The subgroup containing the fixed particle is called the "fixed subgroup," and the others the "unfixed subgroups" (see Fig. 12).

As has been discussed by Hugenholtz,[15] the summation of all possible diagram obtained by ordering a set of disconnected subgroups can be expressed in a simple form as a convolution integral. For example, the summation of the left sides of the Λ lines in diagrams (a) and (b) in Fig. 12 can be expressed as

$$\frac{1}{E_{\mathbf{p}^N} - z} v(q) \frac{1}{E_{\mathbf{p}_1+\hbar\mathbf{q},\mathbf{p}_i-\hbar\mathbf{q},\mathbf{p}^{N-2}} - z} v(q') \frac{1}{E_{\mathbf{p}_1+\hbar\mathbf{q},\mathbf{p}_i-\hbar\mathbf{q},\mathbf{p}_r+\hbar\mathbf{q}',\mathbf{p}_s-\hbar\mathbf{q}',\mathbf{p}^{N-4}} - z}$$

$$+ \frac{1}{E_{\mathbf{p}^N} - z} v(q') \frac{1}{E_{\mathbf{p}_r+\hbar\mathbf{q}',\mathbf{p}_s-\hbar\mathbf{q}',\mathbf{p}^{N-2}} - z}$$

$$\times v(q) \frac{1}{E_{\mathbf{p}_1+\hbar\mathbf{q},\mathbf{p}_i-\hbar\mathbf{q},\mathbf{p}_r+\hbar\mathbf{q}',\mathbf{p}_s-\hbar\mathbf{q}',\mathbf{p}^{N-4}} - z}$$

$$= \frac{1}{E_{\mathbf{p}_1,\mathbf{p}_i} - z} v(q) \frac{1}{E_{\mathbf{p}_1+\hbar\mathbf{q},\mathbf{p}_i-\hbar\mathbf{q}} - z} \circ \frac{1}{E_{\mathbf{p}^{N-2}} - z}$$

$$\times v(q') \frac{1}{E_{\mathbf{p}_r+\hbar\mathbf{q}',\mathbf{p}_s-\hbar\mathbf{q}',\mathbf{p}^{N-4}} - z} \qquad \text{(C2)}$$

where the symbol $\circ$ indicates the convolution integral,

$$f(z) \circ g(z) = \frac{-1}{2\pi i} \int_C d\zeta\, f(z - \zeta) g(\zeta) \qquad \text{(C3)}$$

and the path of integration C is a contour encircling all singular points of the integrand on the real axis, but not encircling the singular points located on the straight line through z parallel to the real axis.

This theorem can be extended to the product of two resolvents $R^{>}(z)R^{<}(z')$ depending on the two complex variables z and z'. Then, the summation of the diagrams (a)–(d) in Fig. 12 is simply expressed by

$$\frac{1}{E_{\mathbf{p}_1,\mathbf{p}_i}-z}v(q)\frac{1}{E_{\mathbf{p}_1+\hbar\mathbf{q},\mathbf{p}_i-\hbar\mathbf{q}}-z}\frac{1}{E_{\mathbf{p}_1+\hbar\mathbf{q},\mathbf{p}_i-\hbar\mathbf{q}}-z'}v(q)\frac{1}{E_{\mathbf{p}_1,\mathbf{p}_i}-z'}$$

$$\circ\frac{1}{E_{\mathbf{p}^{N-2}}-z}v(q')\frac{1}{E_{\mathbf{p}_r+\hbar\mathbf{q}',\mathbf{p}_s-\hbar\mathbf{q}',\mathbf{p}^{N-4}}-z}\frac{1}{E_{\mathbf{p}_r+\hbar\mathbf{q}',\mathbf{p}_s-\hbar\mathbf{q}',\mathbf{p}^{N-4}}-z'}$$

$$v(q')\frac{1}{E_{\mathbf{p}^{N-2}}-z'} \tag{C4}$$

where the symbol $\circ$ indicates the product of the convolution integrals on z and z',

$$f(z)f'(z')\circ g(z)g'(z')=[f(z)\circ g(z)][f'(z')\circ g'(z')] \tag{C5}$$

With the aid of this theorem, we can decompose the product of the two resolvents in (C1) into a convolution integral consisting of the fixed subgroup (f) and unfixed subgroups (uf) as

$$\mathscr{P}R^{>}(z)R^{<}(z')\mathscr{P}=[\mathscr{P}R^{>}(z)R^{<}(z')\mathscr{P}]_{\mathrm{f}}\circ[\mathscr{P}R^{>}(z)R^{<}(z')\mathscr{P}]_{\mathrm{uf}} \tag{C6}$$

The evolution s.operator $\mathscr{U}(t)$, which is the Laplace transform of the product of the two resolvents, is therefore decomposed into a product of evolution s.operators for the fixed subgroup and the unfixed subgroups. Then we get

$$\phi_1(\mathbf{p}_1,t)=(\hbar^3\Omega^{-1})^{N'-1}\sum_{\mathbf{p}^{N'-1}}\sum_{\mathbf{p}'^{N'}}(\mathbf{p}^{N'};\mathbf{p}^{N'}|[\mathscr{U}(t)]_{\mathrm{f}}|\mathbf{p}'^{N'};\mathbf{p}'^{N'})\prod_{i}^{N'}\phi_1(\mathbf{p}_i',0)$$

$$\times(\hbar^3\Omega^{-1})^{N''}\sum_{\mathbf{p}^{N''}}\sum_{\mathbf{p}'^{N''}}(\mathbf{p}^{N''};\mathbf{p}^{N''}|[\mathscr{U}(t)]_{\mathrm{uf}}|\mathbf{p}'^{N''};\mathbf{p}'^{N''})\prod_{j}^{N''}\phi_1(\mathbf{p}_j',0) \tag{C7}$$

where N' is the number of particles in the fixed subgroup and N'' is the number in the unfixed subgroups; $N=N'+N''$. The second factor in (C7) has the same form as (3.30) in the limit $N''\to\infty$. Therefore, all diagrams having potentials cancel through the compensative relation of the diagrams, and only the noninteracting term gives a contribution as unity. Thus, we arrive at the final result,

$$\phi_1(\mathbf{p}_1,t)=(\hbar^3\Omega^{-1})^{N'-1}\sum_{\mathbf{p}^{N'-1}}\sum_{\mathbf{p}'^{N'}}(\mathbf{p}^{N'};\mathbf{p}^{N'}|[\mathscr{U}(t)]_{\mathrm{f}}|\mathbf{p}'^{N'};\mathbf{p}'^{N'})\prod_{i}^{N'}\phi_1(\mathbf{p}_i',0) \tag{C8}$$

where all diagrams on the right-hand side comprise the fixed subgroup. This can be directly extended to more general cases and hence the statement is proved.

ACKNOWLEDGMENTS

The authors would like to express their thanks to Prof. S. Goto for continuous encouragement and to Dr. M. Nakamura for his valuable discussions.

REFERENCES

1. L. Van Hove, *Physica* **23**:441 (1957).
2. I. Prigogine and R. Balescu, *Physica* **25**:281 (1959); **25**:302 (1959); **26**:145 (1960).
3. I. Prigogine, *Non-Equilibrium Statistical Mechanics* (Interscience, New York, 1962).
4. R. Balescu, *Statistical Mechanics of Charged Particles* (Interscience, New York, 1962).
5. I. Prigogine and P. Résibois, *Physica* **27**:629 (1961).
6. G. Severne, *Physica* **31**:877 (1965).
7. I. Prigogine, C. George, and F. Henin, *Physica* **45**:418 (1969).
8. R. Balescu and J. Wallenborn, *Physica* **54**:447 (1971).
9. C. George, I. Prigogine, and L. Rosenfeld, *Mat. Fys. Medd. Dan. Vid. Selsk.* **38**:1 (1972).
10. R. Balescu, *Physica* **56**:1 (1971); **62**:485 (1972).
11. A. Janner, *Helv. Phys. Acta* **35**:47 (1962).
12. R. Swenson, *J. Math. Phys.* **3**:1017 (1962); **4**:544 (1963).
13. N. Mishima and T. Petrosky, *J. Math. Phys.* **19**:1087 (1978).
14. N. Mishima, T. Petrosky, and M. Yamazaki, *J. Stat. Phys.* **14**:359 (1976).
15. N. Hugenholtz, *Physica* **23**:481 (1957).
16. P. Résibois and R. Dagonnier, *Physica* **29**:1057 (1963).